

Dynamical Mean Field Theory and Quantum Cluster Methods

David Sénéchal

Département de physique & Institut Quantique
Université de Sherbrooke

International Summer School on Computational Quantum Materials
June 1, 2016

Outline

- 1 Introduction
- 2 Dynamical Mean Field Theory
- 3 Cluster Perturbation Theory
- 4 Cluster Dynamical Mean Field Theory
- 5 The self-energy functional approach
- 6 Exact Diagonalizations

Outline

- 1 Introduction
- 2 Dynamical Mean Field Theory
- 3 Cluster Perturbation Theory
- 4 Cluster Dynamical Mean Field Theory
- 5 The self-energy functional approach
- 6 Exact Diagonalizations

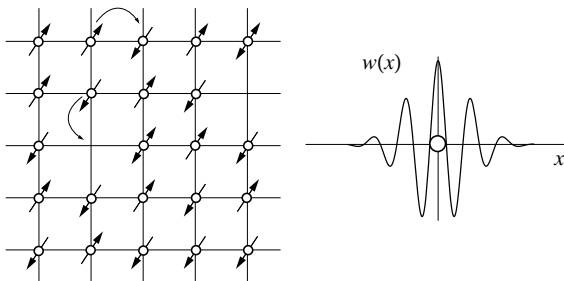
The Hubbard model

Hamiltonian:

$$H = \sum_{r,r',\sigma} t_{r,r'} c_{r\sigma}^\dagger c_{r'\sigma} + U \sum_r n_{r\uparrow} n_{r\downarrow}$$

hopping amplitude ←
creation operator ← → number of spin ↑ electrons at r
→ local Coulomb repulsion

(chemical potential $\mu = -t_{rr}$)



The Green function

- Hilbert space of dimension $\sim 4^L$ (L : # of sites)
- The many-body ground state $|\Omega\rangle$ contains too much information
- A lot of useful information is contained in the one-particle Green function:
(here at $T = 0$)

$\xrightarrow{\text{matrix } \mathbf{G}}$

$$G_{\alpha\beta}(z) = \langle \Omega | c_\alpha \frac{1}{z - H + E_0} c_\beta^\dagger | \Omega \rangle + \langle \Omega | c_\beta^\dagger \frac{1}{z + H - E_0} c_\alpha | \Omega \rangle$$

$\xleftarrow{\text{G.S. energy}}$

- Retarded Green function:

$$G^R(t) = -i\Theta(t) \langle \Omega | \{c_\alpha(t), c_\beta^\dagger(0)\} | \Omega \rangle \implies G^R(\omega) = G(\omega + i0^+)$$

- Approximation schemes for \mathbf{G} are easier to implement

Spectral representation

$$G_{\alpha\beta}(z) = \sum_{r>0} \langle \Omega | c_\alpha | r \rangle \frac{1}{z - E_r + E_0} \langle r | c_\beta^\dagger | \Omega \rangle + \sum_{r<0} \langle \Omega | c_\beta^\dagger | r \rangle \frac{1}{z + E_r - E_0} \langle r | c_\alpha | \Omega \rangle$$

eigenstate with $N+1$ particles ↗
eigenstate with $N-1$ particles ↘

Q-matrix:

$$Q_{\alpha r} = \begin{cases} \langle \Omega | c_\alpha | r \rangle & (r > 0) \\ \langle r | c_\alpha | \Omega \rangle & (r < 0) \end{cases} \quad \text{and} \quad \omega_r = \begin{cases} E_r - E_0 & (r > 0) \\ E_0 - E_r & (r < 0) \end{cases}$$

Spectral representation:

$$G_{\alpha\beta}(z) = \sum_r \frac{Q_{\alpha r} Q_{\beta r}^*}{z - \omega_r}$$

(partial fractions)

Spectral representation (cont.)

Completeness relations:

$$\sum_r Q_{\alpha r} Q_{\beta r}^* = \langle \Omega | (c_\alpha c_\beta^\dagger + c_\beta^\dagger c_\alpha) | \Omega \rangle \\ = \delta_{\alpha\beta}$$

Asymptotic behavior:

$$\lim_{z \rightarrow \infty} G_{\alpha\beta}(z) = \frac{\delta_{\alpha\beta}}{z}$$

Spectral function

Spectral function:

$$A_{\alpha\beta}(\omega) = -2 \operatorname{Im} G_{\alpha\beta}(\omega + i0^+)$$

Translation-invariant system:

$$G(k, z) = \sum_{r>0} |\langle \Omega | c_k | r \rangle|^2 \frac{1}{z - E_r + E_0} + \sum_{r<0} |\langle \Omega | c_k^\dagger | r \rangle|^2 \frac{1}{z + E_r - E_0}$$

$$\begin{aligned} A(k, \omega) &= -2 \operatorname{Im} G(k, \omega + i0^+) \\ &= \sum_{r>0} |\langle \Omega | c_k | r \rangle|^2 2\pi\delta(\omega - E_r + E_0) \\ &\quad + \sum_{r<0} |\langle \Omega | c_k^\dagger | r \rangle|^2 2\pi\delta(\omega + E_r - E_0) \end{aligned}$$

prob. of electron
with $\varepsilon = E_r - E_0$ ←
prob. of hole
with $\varepsilon = E_r - E_0$

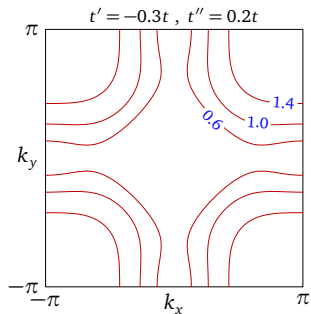
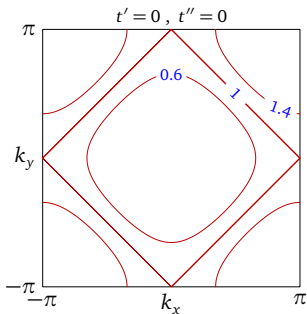
non-interacting limit ($U = 0$)

$$|\Omega\rangle = \prod_{\epsilon_k < 0} c_k^\dagger |0\rangle \quad (\text{Fermi sea})$$

$$G(z) = \frac{1}{z - t}$$

$$G(z, k) = \frac{1}{z - \varepsilon_k}$$

$$\varepsilon_k = \sum_r t_{0,r} e^{-ik \cdot r}$$

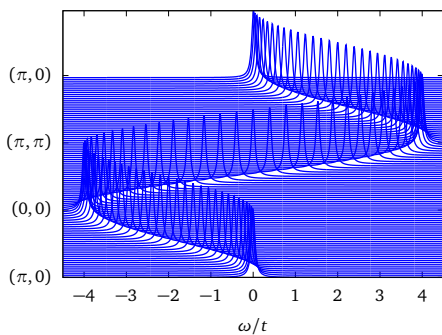


non-interacting limit (cont.)

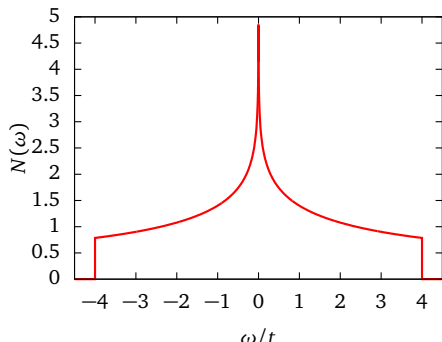
Spectral function & density of states:

$$A(k, \omega) = 2\pi\delta(\omega - \varepsilon_k)$$

$$\rho(\omega) = \int_k A(k, \omega)$$



Spectral function, half-filling, NN hopping



Associated density of states

Self-energy

Interacting Green function:

$$G(z) = \frac{1}{z - t - \Sigma(z)}$$

\hookrightarrow self-energy

Local limit at half-filling ($t = -\frac{1}{2}U\mathbf{1}$):

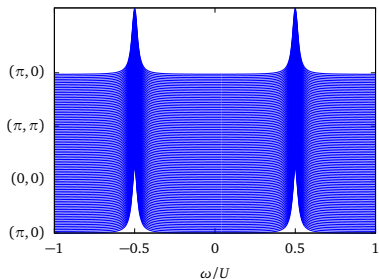
$$G(z) = \frac{1/2}{z + U/2} + \frac{1/2}{z - U/2} = \frac{1}{z - \frac{U^2}{4z}}$$

$$\Sigma(z) = \frac{U^2}{4z} + \frac{U}{2}$$

Analytic structure:

$$\Sigma_{\alpha\beta}(z) = \Sigma_{\alpha\beta}^{\infty} + \sum_r \frac{S_{\alpha r} S_{\beta r}^*}{z - \sigma_r}$$

Hartree-Fock \hookleftarrow



Spectral function, half-filled HM ($t = 0$)

Outline

1 Introduction

2 Dynamical Mean Field Theory

- Approximation schemes
- The cavity method
- The hybridization function
- The self-consistency condition
- Impurity solvers
- The Mott transition

3 Cluster Perturbation Theory

4 Cluster Dynamical Mean Field Theory

5 The self-energy functional approach

Approximation schemes

Hartree-Fock

- $\Sigma(\omega, k) \rightarrow \Sigma(\infty, k)$ is frequency-independent
- Can be absorbed in new dispersion relation $\varepsilon'(k)$
- Approximation equivalent to new one-body Hamiltonian

DMFT

- $\Sigma(\omega, k) \rightarrow \Sigma(\omega)$ is momentum-independent
- System still fundamentally interacting
- Approximated by single site with effective medium

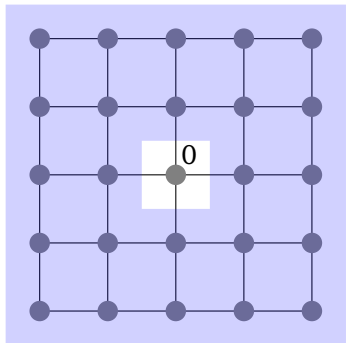
The cavity method

Action of the Hubbard model:

$$S[c_{r\sigma}, c_{r\sigma}^\dagger] = \int_0^\beta d\tau \left\{ \sum_{r,\sigma} c_{r\sigma}^\dagger \partial_\tau c_{r\sigma} + \sum_{r,r',\sigma} t_{rr'} c_{r\sigma}^\dagger c_{r'\sigma} + U \sum_r n_{r\uparrow} n_{r\downarrow} \right\}$$

One-site effective action:

$$\begin{aligned} \frac{1}{Z_{\text{eff.}}} e^{-S_{\text{eff.}}} [c_{0\sigma}, c_{0\sigma}^\dagger] \\ = \frac{1}{Z} \int \prod_{r \neq 0, \sigma} \mathcal{D}c_{r\sigma} \mathcal{D}c_{r\sigma}^\dagger e^{-S} \end{aligned}$$



The cavity method (cont.)

Effective action (exact form, spin indices suppressed):

$$S_{\text{eff.}} = S_0 + \sum_{n=1}^{\infty} \sum_{r_1, \dots, r'_n} \int d\tau \eta_{r_1}^\dagger \cdots \eta_{r_n}^\dagger \eta_{r'_1} \cdots \eta_{r'_n} G_{r_1 \dots r'_n}^{\text{env}}(\tau_1 \cdots \tau_{r_n}, \tau_1 \cdots \tau_n)$$

where $\eta_r = t_{r0} c_{r0}$ acts like a source field and

$$S_0 = \int_0^\beta d\tau \left\{ c_0 \partial_\tau c_0 - \mu n_0 + U n_{0\uparrow} n_{0\downarrow} \right\}$$

One can show that in the $d \rightarrow \infty$ limit, if $t \rightarrow t/\sqrt{2d}$, only $n = 1$ survives.
DMFT approximation:

$$S_{\text{eff.}} = S_0 + \sum_{r,r'} t_{0r} t_{0r'} \int d\tau d\tau' c_0^\dagger(\tau) c_0(\tau') G_{r,r'}^{\text{env}}(\tau, \tau')$$

The cavity method (cont.)

Effective action:

$$S_{\text{eff.}} = - \int d\tau d\tau' c_0^\dagger(\tau) \mathcal{G}_0^{-1}(\tau - \tau') c_0(\tau') + U \int_0^\beta d\tau n_{0\uparrow} n_{0\downarrow}$$
$$\mathcal{G}_0^{-1}(i\omega_n) = i\omega_n + \mu - \sum_{r,r'} t_{0r} t_{0r'} G_{r,r'}^{\text{env}}(i\omega_n)$$

- $G_{r,r'}^{\text{env}}(i\omega_n)$ unknown.
Rather, treat \mathcal{G}_0^{-1} as an adjustable **dynamical mean field**
- Only single particles hop on and off the site
- The environment is uncorrelated
- Nonlocal in time: no Hamiltonian involving c_0 only

The hybridization function

- \mathcal{G}_0 has the analytic properties of a Green function: poles on the real axis and positive residues.
- Define the **hybridization function** $\Gamma(z)$:

$$\mathcal{G}_0^{-1}(z) = z + \mu - \Gamma(z)$$

- $\Gamma(z)$ has the analytic properties of a self-energy and can be represented by a (quasi-infinite) set of poles:

$$\Gamma(z) = \sum_r \frac{\theta_r^2}{z - \epsilon_r}$$

- Interacting Green function of the effective theory for the ‘single site’:

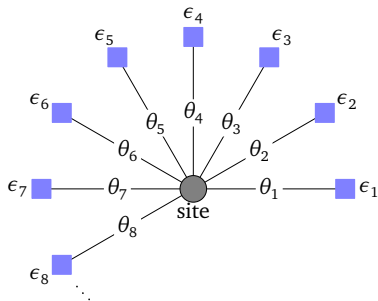
$$G_s(z) = \frac{1}{z + \mu - \Gamma(z) - \Sigma(z)}$$

Hamiltonian representation

G_s can be obtained from the following AIM Hamiltonian:

$$H_{\text{AIM}} = \sum_{r=1}^{N_b} \theta_r (c_0^\dagger a_r + \text{H.c.}) + \sum_{r=1}^{N_b} \epsilon_r a_r^\dagger a_r - \mu c_0^\dagger c_0 + U n_{0\uparrow} n_{0\downarrow}$$

hyb. amplitude ← ↗ bath orbital ↗ bath energy



One-body matrix:

$$T = \begin{pmatrix} -\mu & \boldsymbol{\theta}_{[1 \times N_b]} \\ \boldsymbol{\theta}_{[N_b \times 1]}^\dagger & \boldsymbol{\epsilon}_{[N_b \times N_b]} \end{pmatrix}$$

Proof ($U = 0$)

$$G_{\text{full}}(z) = \begin{pmatrix} G_s & G_{sb} \\ G_{bs} & G_b \end{pmatrix} \quad G_{\text{full}}^{-1}(z) = z - T = \begin{pmatrix} z + \mu & -\theta \\ -\theta^\dagger & z - \varepsilon \end{pmatrix}$$

Need to invert a block matrix:

$$\begin{pmatrix} z + \mu & -\theta \\ -\theta^\dagger & z - \varepsilon \end{pmatrix} \begin{pmatrix} G_s & G_{sb} \\ G_{bs} & G_b \end{pmatrix} = \mathbf{1}$$

block equations:

$$(z + \mu)G_s - \theta G_{bs} = \mathbf{1} \quad \text{and} \quad -\theta^\dagger G_s + (z - \varepsilon)G_{bs} = 0$$

$$G_{bs} = (z - \varepsilon)^{-1} \theta^\dagger G_s \implies \left[(z + \mu) - \theta \frac{1}{z - \varepsilon} \theta^\dagger \right] G_s = \mathbf{1}$$

therefore

$$G_s^{-1} = z + \mu - \theta \frac{1}{z - \varepsilon} \theta^\dagger = z + \mu - \Gamma(z)$$

Proof (cont.)

where

$$\Gamma(z) = \theta \frac{1}{z - \epsilon} \theta^\dagger = \sum_{r=1}^{N_b} \frac{\theta_r^2}{z - \epsilon_r}$$

If $U \neq 0$, simply add the self-energy:

$$G_s(z) = \frac{1}{z + \mu - \Gamma(z) - \Sigma(z)}$$

The self-consistency condition

- Lattice model Green function in the DMFT approximation:

$$G(i\omega_n, k) = \frac{1}{i\omega_n - \varepsilon(k) - \Sigma(i\omega_n)}$$

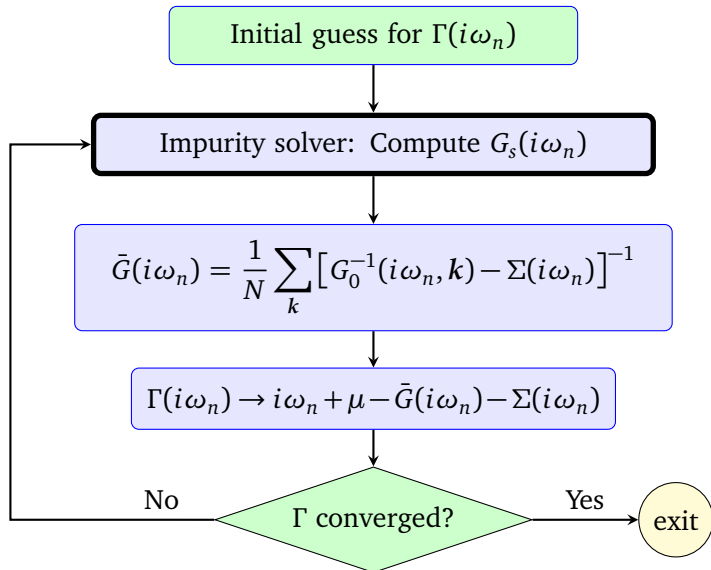
- The local Green function

$$\bar{G}(i\omega_n) = \frac{1}{N} \sum_k G(i\omega_n, k)$$

must coincide with $G_s(i\omega_n)$:

$$\begin{aligned}\bar{G}(i\omega_n)^{-1} &= i\omega_n + \mu - \Gamma(i\omega_n) - \Sigma(i\omega_n) \\ &= \mathcal{G}_0^{-1}(i\omega_n) - \Sigma(i\omega_n)\end{aligned}$$

The DMFT self-consistency loop



The impurity solver

Methods for solving the impurity Hamiltonian:

- Perturbation theory (2nd order, NCA)
- Numerical Renormalization Group (NRG)
- Quantum Monte Carlo (QMC)
 - Infinite bath: only $\Gamma(i\omega_n)$ is needed.
 - Finite temperature
 - **Hirsch-Fye** (time grid) or **Continuous-time** (no discretization error)
 - But: sign problem
- Exact diagonalizations
 - restricted to small, discrete baths (explicit form of H_{AIM})
Hence self-consistency relation only approximately satisfied
 - real-frequency information
 - zero temperature
- Other real frequency methods: CI, natural basis, etc.

The DMFT self-consistency loop (discrete bath version)

- 1 Start with a guess value of $(\theta_r, \varepsilon_r)$
- 2 Compute the impurity Green function $G_s(i\omega_n)$ (ED)
- 3 Compute the lattice-averaged (or local) Green function

$$\bar{G}(i\omega_n) = \frac{1}{N} \sum_k \frac{1}{G_0^{-1}(k) - \Sigma(i\omega_n)} \quad \text{and} \quad \mathcal{G}_0^{-1}(i\omega_n) = \bar{G}^{-1} + \Sigma(i\omega_n)$$

- 4 Minimize the following **distance function**:

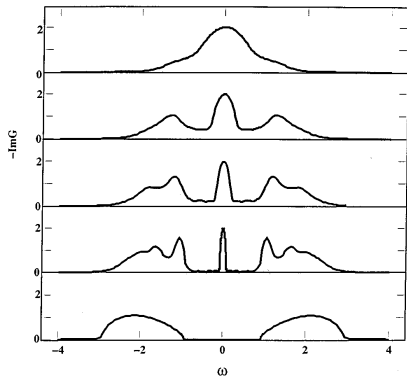
$$d(\boldsymbol{\theta}, \boldsymbol{\varepsilon}) = \sum_{\omega_n} W(i\omega_n) \text{tr} \left| G_s^{-1}(i\omega_n) - \bar{G}^{-1}(i\omega_n) \right|^2$$

↳ weights

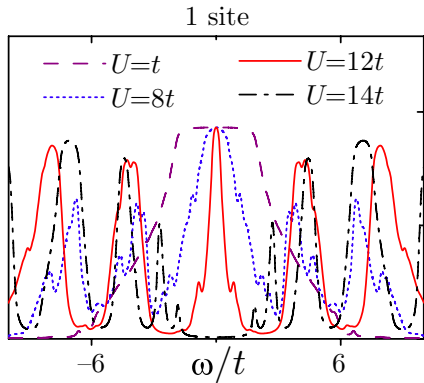
over the set of bath parameters. Thus obtain a new set $(\theta_r, \varepsilon_r)$.

- 5 Go back to step (2) until convergence.

Application: The Mott transition

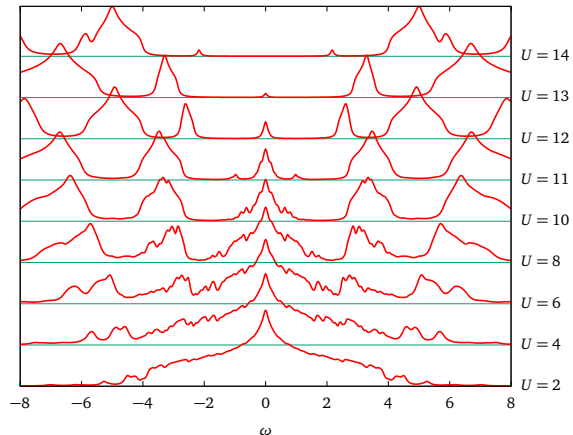


Density of states $N(\omega)$ for the half-filled Hubbard model on the Bethe lattice with interactions $U/D = 1, 2, 2.5, 3, 4$. Iterated perturbation theory. Zhang et al., Phys. Rev. Lett. 70, 1666 (1993).

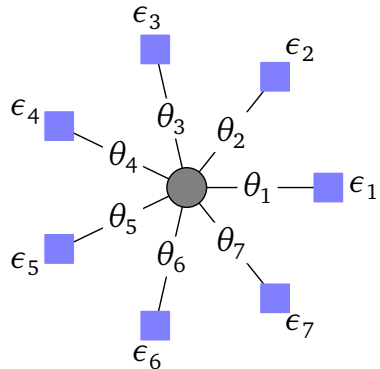


$N(\omega)$ for the half-filled 3D Hubbard model. Exact diagonalization solver. Zhang and Imada, Phys. Rev. B 76, 045108 (2007).

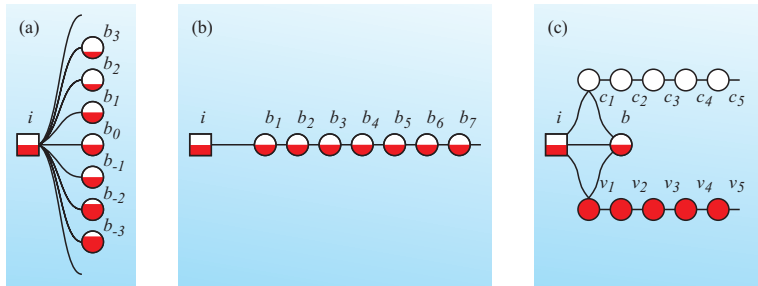
The Mott transition (cont.)



$N(\omega)$ in the 2D, half-filled Hubbard model. Exact diagonalization solver with $N_b = 7$.

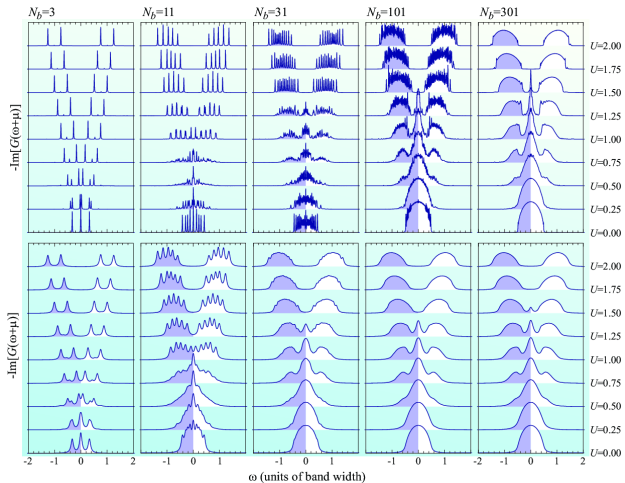


Breaking the exponential barrier



Lu et al., Phys. Rev. B90, 085102 (2014).

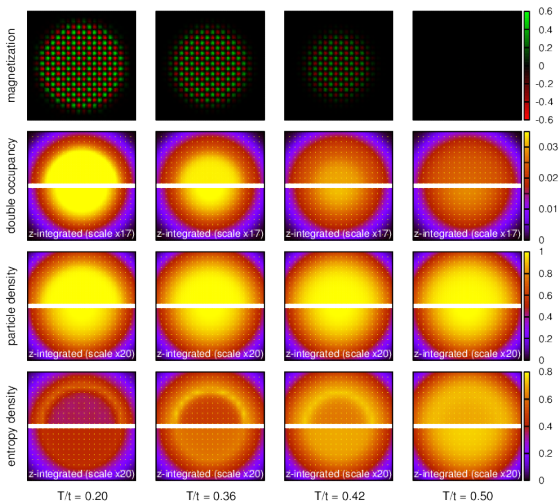
Breaking the exponential barrier (cont.)



Real-space DMFT : Ultra-cold atoms

Antiferromagnetic order in cold atom systems with harmonic trap

$$H = \sum_{\mathbf{r}, \mathbf{r}', \sigma} t_{\mathbf{r}, \mathbf{r}'} c_{\mathbf{r}\sigma}^\dagger c_{\mathbf{r}'\sigma} + U \sum_{\mathbf{r}} n_{\mathbf{r}\uparrow} n_{\mathbf{r}\downarrow} - \sum_{\mathbf{r}, \sigma} (V_{\mathbf{r}} - \mu) n_{\mathbf{r}, \sigma}$$



Outline

- 1 Introduction
- 2 Dynamical Mean Field Theory
- 3 Cluster Perturbation Theory
 - kinematics
 - CPT : examples
- 4 Cluster Dynamical Mean Field Theory
- 5 The self-energy functional approach
- 6 Exact Diagonalizations

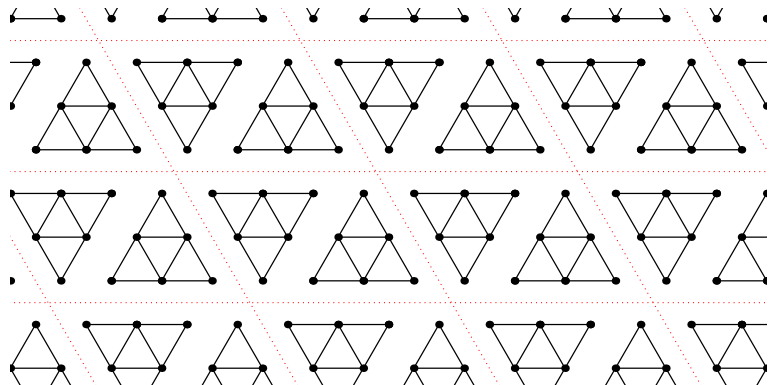
Real-space cluster methods: General idea

- Tile the lattice with small units (clusters)
- Solve an approximate, effective problem on each cluster
- Use the self-energies $\Sigma^{(j)}(z)$ to approximate the full self-energy:

$$\Sigma = \begin{pmatrix} \Sigma^{(1)} & 0 & \cdots & 0 \\ 0 & \Sigma^{(2)} & \cdots & 0 \\ \vdots & \vdots & \ddots & \vdots \\ 0 & 0 & \cdots & \Sigma^{(n)} \end{pmatrix}$$

- Varieties:
 - **CPT** : Cluster Perturbation Theory
 - VCA : Variational Cluster Approximation
 - **CDMFT** : Cluster Dynamical Mean Field Theory
 - CDIA : Cluster Dynamical Impurity Approximation

Tiling the lattice into clusters



Tiling of the triangular lattice with 6-site clusters

Cluster Perturbation Theory

Cluster decomposition of the one-body matrix:

$$t = \begin{pmatrix} t^{(1,1)} & t^{(1,2)} & \dots & t^{(1,n)} \\ t^{(2,1)} & t^{(2,2)} & \dots & t^{(2,n)} \\ \vdots & \vdots & \ddots & \vdots \\ t^{(n,1)} & t^{(n,2)} & \dots & t^{(n,n)} \end{pmatrix}$$

↗ diagonal blocks

$$t = t' + t_{\text{ic}}$$

Cluster Green function:

$$G^{(j)-1}(z) = z - t^{(j,j)} - \Sigma^{(j)}(z)$$

CPT Green function for the full system:

$$G_{\text{cpt}}^{-1}(z) = \bigoplus_j G^{(j)-1}(z) - t_{\text{ic}}$$

↗ inter-cluster blocks

Cluster Perturbation Theory (cont.)

lattice Hamiltonian \leftarrow \rightarrow cluster Hamiltonian

$$H = H' + H_{\text{ic}} \quad H_{\text{ic}} = \sum_{\alpha, \beta} (t_{\text{ic}})_{\alpha \beta} c_{\alpha}^{\dagger} c_{\beta}$$

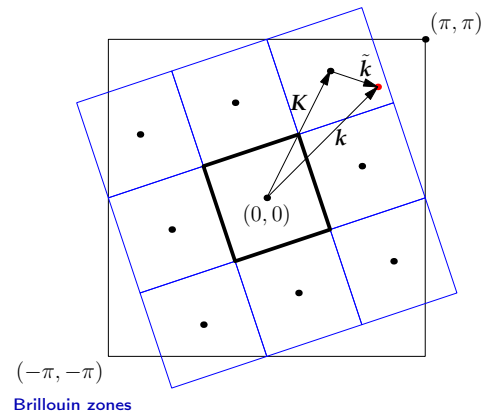
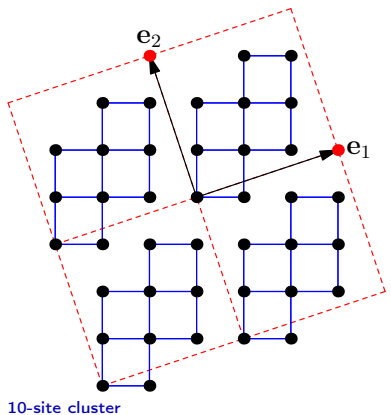
- Treat H_{ic} at lowest order in Perturbation theory
- At this order, the Green function is

$$G^{-1}(z) = G'^{-1}(z) - t_{\text{ic}} \quad \downarrow \text{cluster Green function matrix}$$

C. Gros and R. Valenti, Phys. Rev. B **48**, 418 (1993)

D. Sénéchal, D. Perez, and M. Pioro-Ladrière. Phys. Rev. Lett. **84**, 522 (2000)

Superlattices and reduced Brillouin zones



CPT for translation invariant tilings

site within cluster \leftarrow \rightarrow reduced wavevector

one-body index = (R, \tilde{k}, σ)

\hookrightarrow spin (or band)

Green function and t_{ic} are diagonal in \tilde{k} .

G' is independent of k .

The CPT formula may be written as

$$G^{-1}(z, \tilde{k}) = G'^{-1}(z) - t_{ic}(\tilde{k})$$

where matrices are now in (R, σ) space.

Interlude : Fourier transforms

Unitary matrices performing Fourier transforms:

$$U_{k,r}^\gamma = \frac{1}{\sqrt{N}} e^{-ik \cdot r} \quad U_{\tilde{k}\tilde{r}}^\Gamma = \sqrt{\frac{L}{N}} e^{-i\tilde{k} \cdot \tilde{r}} \quad U_{K,R}^c = \frac{1}{\sqrt{L}} e^{-iK \cdot R}$$

complete superlattice cluster

Various representations of the annihilation operator

$$c(k) = \sum_r U_{kr}^\gamma c_r \quad c_K(\tilde{k}) = \sum_{\tilde{r},R} U_{\tilde{k}\tilde{r}}^\Gamma U_{KR}^c c_{\tilde{r}+R}$$
$$c_R(\tilde{k}) = \sum_{\tilde{r}} U_{\tilde{k}\tilde{r}}^\Gamma c_{\tilde{r}+R} \quad c_{\tilde{r},K} = \sum_R U_{KR}^c c_{\tilde{r}+R}$$

Caveat: $\mathbf{U}^\gamma \neq \mathbf{U}^\Gamma \otimes \mathbf{U}^c$

The matrix $\Lambda = \mathbf{U}^\gamma (\mathbf{U}^\Gamma \otimes \mathbf{U}^c)^{-1}$ relates (K, \tilde{k}) to k :

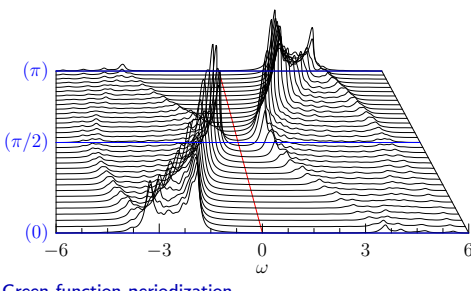
$$c(\tilde{k} + K) = \Lambda_{K,K'}(\tilde{k}) c_{K'}(\tilde{k})$$

Periodization

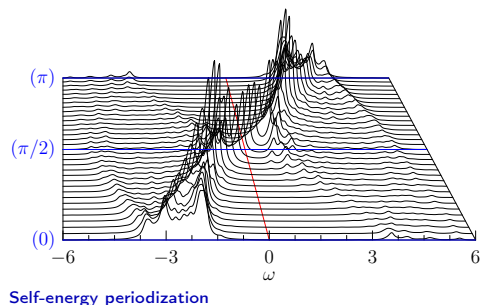
- CPT breaks translation invariance, which needs to be restored:

$$G_{\text{per.}}(k, z) = \frac{1}{L} \sum_{R, R'} e^{-ik \cdot (R - R')} G_{RR'}(\tilde{k}, z)$$

- Periodizing (1D half-filled HM, 12-site cluster):



Green function periodization



Self-energy periodization

Periodization (2)

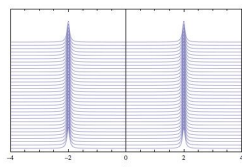
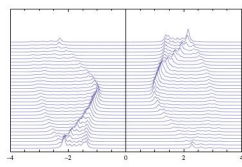
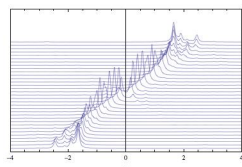
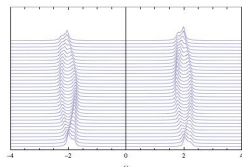
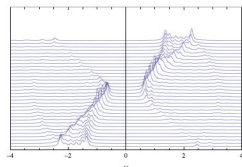
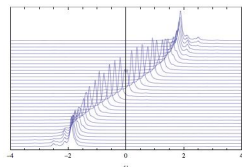
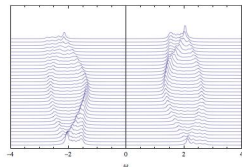
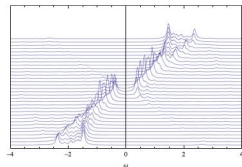
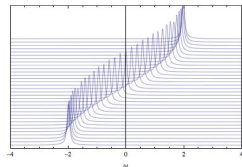
- Periodization as a change of basis:

$$\begin{aligned} G(\tilde{k} + K, \tilde{k} + K', z) &= (\Lambda^c(\tilde{k}) G(z) \Lambda^{c\dagger}(\tilde{k}))_{KK'} \\ &= \frac{1}{L^2} \sum_{R, R', K_1, K'_1} e^{-i(\tilde{k} + K - K_1) \cdot R} e^{i(\tilde{k} + K' - K'_1) \cdot R'} G_{K_1 K'_1}(z) \\ &= \frac{1}{L} \sum_{R, R'} e^{-i(\tilde{k} + K) \cdot R} e^{i(\tilde{k} + K') \cdot R'} G_{RR'}(\tilde{k}, z) \end{aligned}$$

- Set $K = K'$: the spectral function is a partial trace and thus involves diagonal elements only
- Replace \tilde{k} by $k = \tilde{k} + K$ in $G_{RR'}(\tilde{k}, z)$, which leaves $t_{ic}(\tilde{k})$ unchanged
- Since this is a change of basis, analytic properties are still OK.

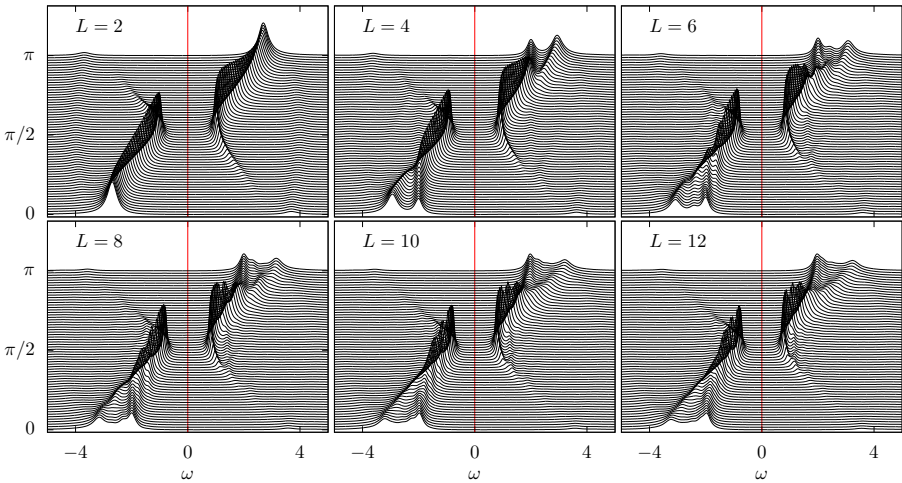
One-dimensional example

Spectral function of the half-filled HM with increasing U/t :



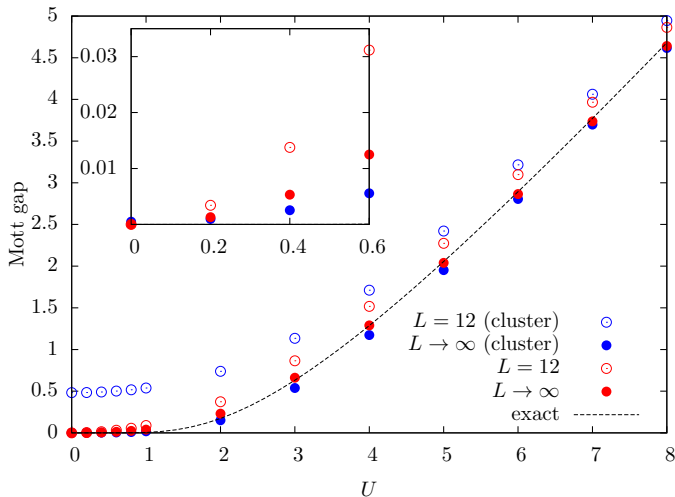
One-dimensional example (cont.)

Spectral function of the half-filled HM with increasing L at $U = 4t$:

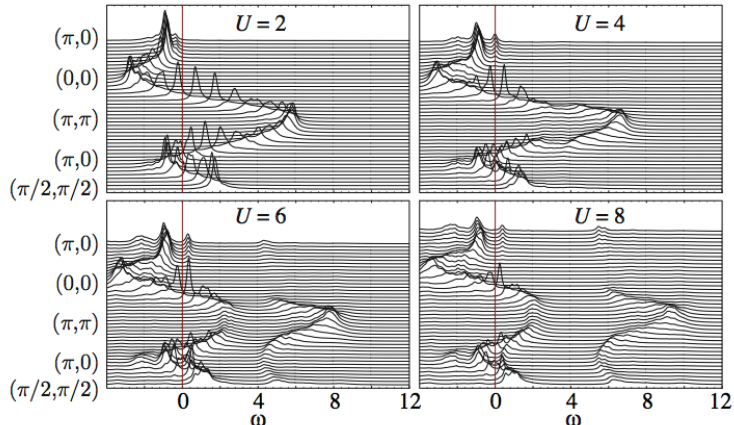


One-dimensional example (cont.)

Spectral gap at half-filling: periodic cluster vs CPT

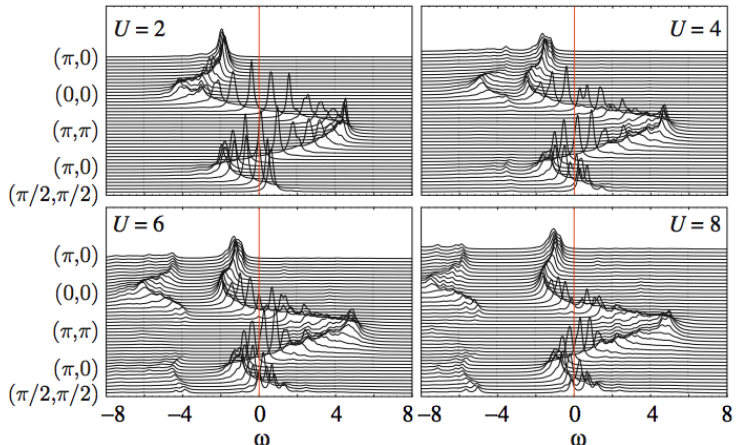


Application: Pseudogap in h-doped cuprates



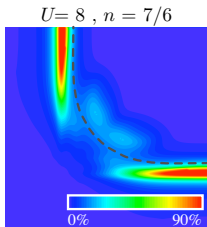
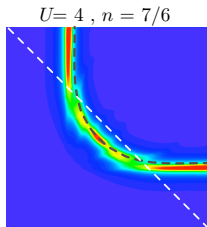
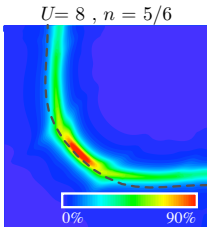
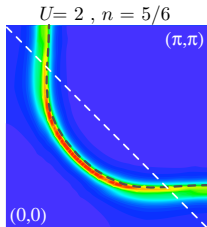
2D Hubbard model, $t' = -0.3t$, $t'' = 0.2t$, 3×4 cluster, $n = 5/6$
Sénéchal and Tremblay, PRL 92, 126401 (2004)

Application: Pseudogap in e-doped cuprates

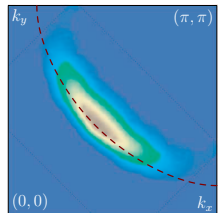


2D Hubbard model, $t' = -0.3t$, $t'' = 0.2t$, 3×4 cluster, $n = 7/6$
Sénéchal and Tremblay, PRL 92, 126401 (2004)

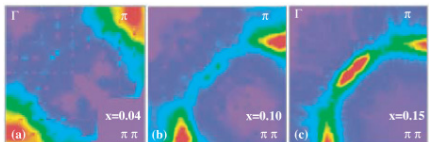
Application: Fermi surface maps



Sénéchal and Tremblay, PRL 92, 126401 (2004)



F. Ronning et al., PRB 67, 165101 (2003)



N.P. Armitage et al., PRL 88, 257001 (2002)

CPT : Conclusion

- Approximation scheme for the one-body Green function
 - Yields approximate values for the averages of one-body operators
- Exact at $U = 0$
- Exact at $t_{ij} = 0$
- Exact short-range correlations
- Allows all values of the wavevector
- Controlled by the size of the cluster
- But :
 - No long-range order, no self-consistency
 - Higher Green functions still confined to the cluster

⇒ A first step towards CDMFT or VCA

Outline

1 Introduction

2 Dynamical Mean Field Theory

3 Cluster Perturbation Theory

4 Cluster Dynamical Mean Field Theory

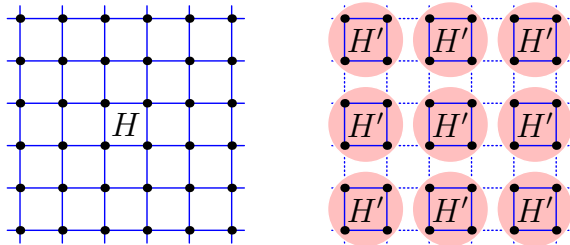
- The hybridization function
- The CDMFT self-consistency condition
- Applications
- The Dynamical Cluster Approximation (DCA)

5 The self-energy functional approach

6 Exact Diagonalizations

Generalization of DMFT to small clusters

- $H_{\text{AIM}} \rightarrow H'$
- Simple adaptation of DMFT
- Scalar equations
→ matrix equations



Dynamical mean field \mathcal{G}_0 :

$$S_{\text{eff}}[c, c^*] = - \int_0^\beta d\tau d\tau' \sum_{\alpha, \beta} c_\alpha^*(\tau) \mathcal{G}_{0, \alpha\beta}^{-1}(\tau - \tau') c_\beta(\tau') + \int_0^\beta d\tau H_1(c, c^*)$$

The hybridization function

In the frequency domain:

$$\mathcal{G}_0^{-1}(i\omega_n) = i\omega_n - \mathbf{t}' - \Gamma(i\omega_n) \quad \text{where} \quad \mathcal{G}_0(i\omega_n) = \int_0^\beta e^{i\omega_n \tau} \mathcal{G}_0(\tau)$$

↗ hybridization function

Spectral representation of Γ :

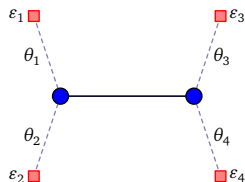
$$\Gamma_{\alpha\beta}(i\omega_n) = \sum_r^{N_b} \frac{\theta_{ar} \theta_{\beta r}^*}{i\omega_n - \varepsilon_r} = \boldsymbol{\theta} \frac{1}{i\omega_n - \boldsymbol{\varepsilon}} \boldsymbol{\theta}^\dagger$$

Corresponding Hamiltonian:

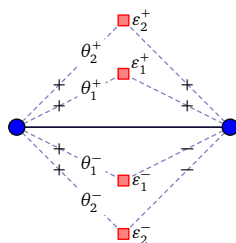
$$H' = \sum_{\alpha, \beta} t'_{\alpha\beta} c_\alpha^\dagger c_\beta + U \sum_i n_{i\uparrow} n_{i\downarrow} + \sum_{r, \alpha} \theta_{ra} (c_\alpha^\dagger a_r + \text{H.c.}) + \sum_r \varepsilon_r a_r^\dagger a_r$$

hybridization matrix ↗ bath orbital ↗
bath energies ↘

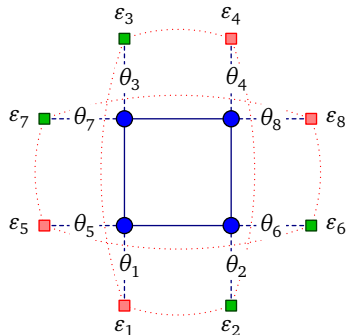
Discrete bath systems



(A)



(B)



(C)

(B) : Liebsch and Ishida, Journal of Physics: Condensed Matter 24 (2012), no. 5, 053201.

The CDMFT Procedure (discrete bath)

- 1 Start with a guess value of $(\theta_{ar}, \varepsilon_r)$.
- 2 Calculate the cluster Green function $G'(\omega)$ (ED).
- 3 Calculate the superlattice-averaged Green function

$$\bar{G}(\omega) = \sum_{\tilde{k}} \frac{1}{G_0^{-1}(\tilde{k}) - \Sigma(\omega)} \quad \text{and} \quad \mathcal{G}_0^{-1}(\omega) = \bar{G}^{-1} + \Sigma(\omega)$$

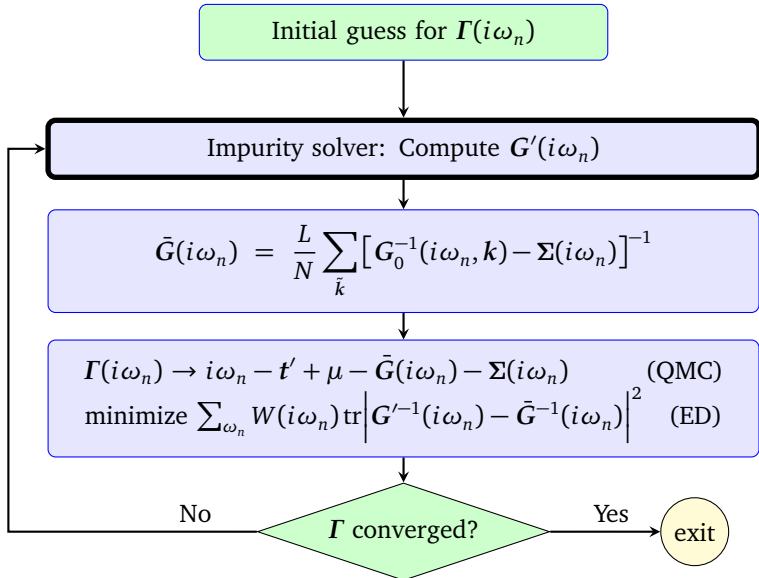
- 4 Minimize the following distance function:

$$d(\boldsymbol{\theta}, \boldsymbol{\varepsilon}) = \sum_{\omega_n} W(i\omega_n) \operatorname{tr} \left| G'^{-1}(i\omega_n) - \bar{G}^{-1}(i\omega_n) \right|^2$$

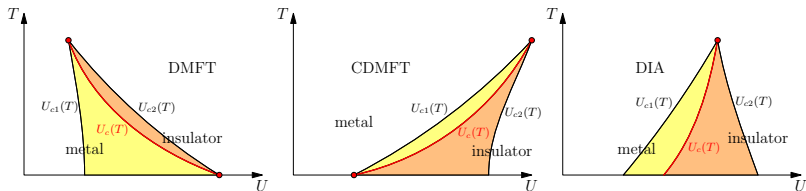
over the set of bath parameters. Thus obtain a new set $(\theta_{ar}, \varepsilon_r)$.

- 5 Go back to step (2) until convergence.

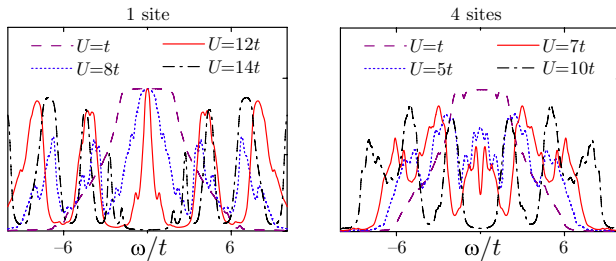
The CDMFT self-consistency loop



Application: The Mott transition

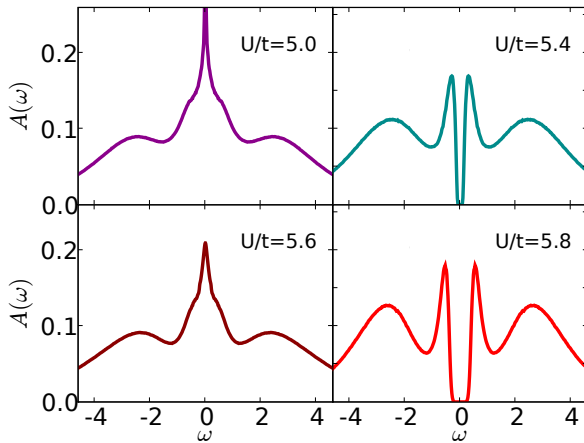


M. Balzer et al., *Europhys. Lett.* 85, 17002 (2009)

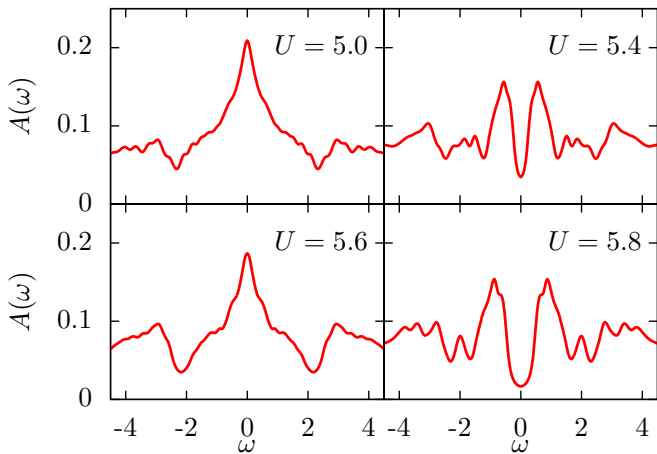


Y.Z. Zhang, M. Imada, *Phys. Rev. B* 76, 045108 (2007)

Application: the Mott transition (QMC)



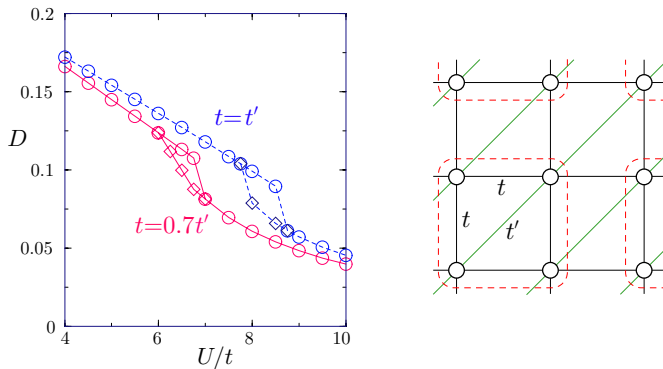
Application: the Mott transition (ED)



solutions from M. Balzer et al., Europhys. Lett. 85, 17002 (2009)

First-order character of the Mott transition (CDMFT)

- The Mott transition is seen in CDMFT as a hysteresis of the double occupancy
- This shows up nicely in a simulation of BEDT organic superconductors



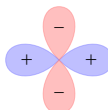
Digression: Superconductivity

- Superconductivity is described by pairing fields:

$$\Delta = \sum_{r,r'} \Delta_{rr'} c_{r\uparrow} c_{r'\downarrow} + \text{H.c}$$

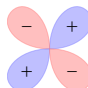
- s -wave pairing: $\Delta_{rr'} = \delta_{rr'}$
- $d_{x^2-y^2}$ pairing:

$$\Delta_{rr'} = \begin{cases} 1 & \text{if } r - r' = \pm x \\ -1 & \text{if } r - r' = \pm y \end{cases}$$



- d_{xy} pairing:

$$\Delta_{rr'} = \begin{cases} 1 & \text{if } r - r' = \pm(x + y) \\ -1 & \text{if } r - r' = \pm(x - y) \end{cases}$$



- Pairing fields are introduced in the bath, and measured on the cluster

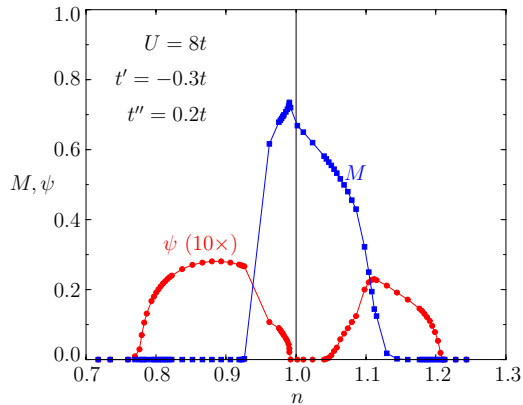
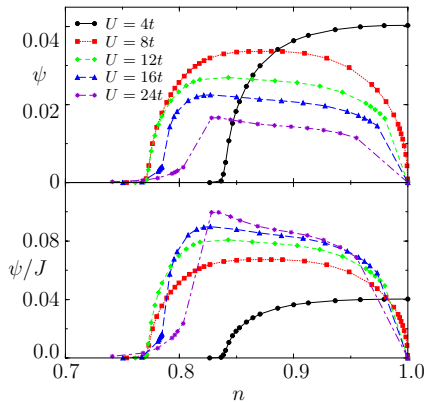
Digression: Superconductivity (cont.)

- Pairing fields violate particle number conservation
- The Hilbert space is enlarged to encompass all particle numbers with a given total spin
- Use the **Nambu formalism**: a particle-hole transformation on the spin-down sector: $c_{\alpha\downarrow} \rightarrow c_{\alpha\downarrow}^\dagger$ and $a_{r\downarrow} \rightarrow a_{r\downarrow}^\dagger$
- Structure of the one-body matrix:

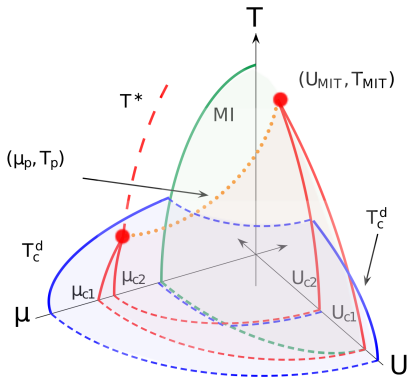
$$\begin{pmatrix} c_\uparrow & \begin{pmatrix} t_\uparrow & \theta_\uparrow & 0 & 0 \\ \theta_\uparrow^\dagger & \varepsilon_\uparrow & 0 & \Delta_b \\ 0 & 0 & -t_\downarrow & -\theta_\downarrow \\ 0 & \Delta_b^\dagger & -\theta_\downarrow^\dagger & -\varepsilon_\downarrow \end{pmatrix} \\ a_\uparrow^\dagger & \end{pmatrix}$$

Application: dSC and AF in the 2D Hubbard model

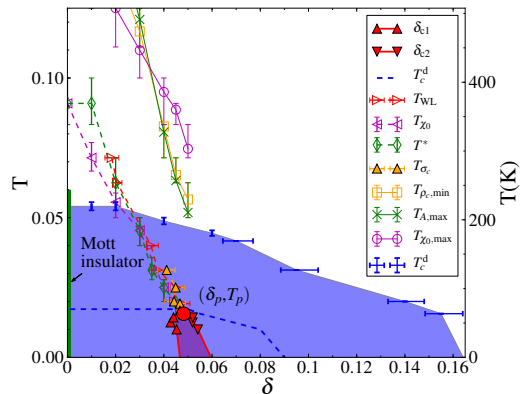
- Nine bath parameters
- Homogeneous coexistence of $d_{x^2-y^2}$ SC and Néel AF



Mott transition and superconductivity



Sordi et al., Phys. Rev. Lett. **108** (2012), 216401



P. Semon et al., Phys. Rev. B **89**, 165113 (2014)

Mott transition and superconductivity (cont.)

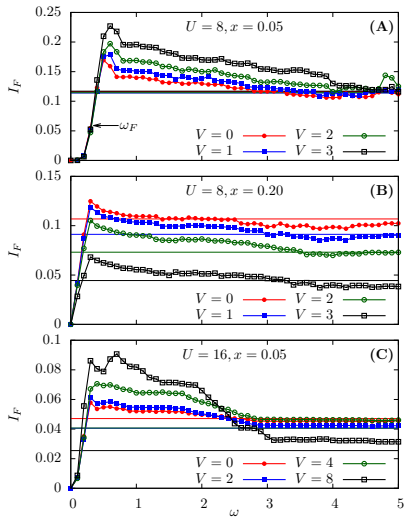
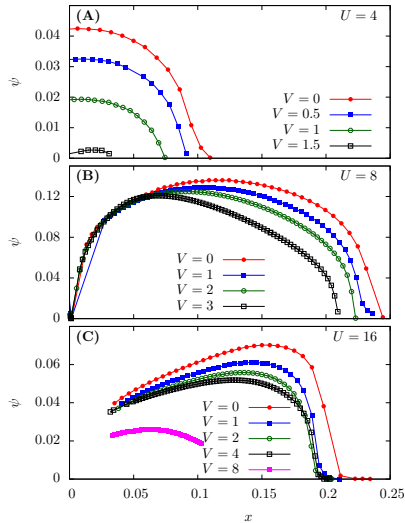
- First-order, finite-doping transition with finite- T critical point: correlated metal vs pseudogap phase.
- The pseudogap phenomenon is related to the Widom line in first-order transitions
- Even though the SC order parameter is suppressed by the Mott transition, T_c isn't
- Results obtained with an efficient CT-QCM-HYB solver.

Application: Resilience of dSC to extended interactions

$$H = \sum_{r,r',\sigma} t_{r,r'} c_{r\sigma}^\dagger c_{r'\sigma} + U \sum_r n_{r\uparrow} n_{r\downarrow} + \sum_{r \neq r'} V_{rr'} \textcolor{red}{n_r n_{r'}} - \mu \sum_{r,\sigma} n_{r,\sigma}$$

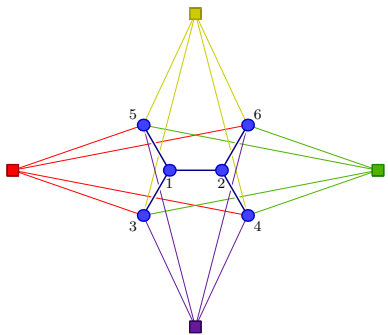
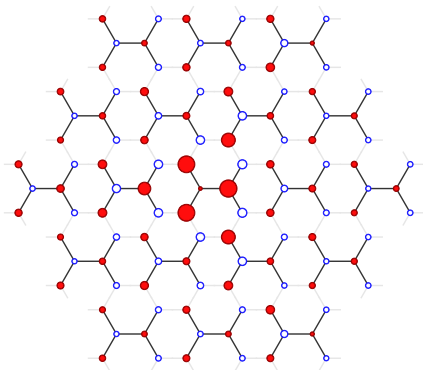
- Question: effect of NN repulsion V on dSC in the 2D Hubbard model?
 - V is a priori detrimental to dSC (pair breaking effect), and larger than J .
 - But: V increases J .
- Exact treatment of V within the cluster; Hartree approximation between clusters.
- Result: a moderate V has no effect on dSC at low doping.
- The retarded nature of the effective pairing interaction is important.

Resilience of dSC to extended interactions (cont.)



Non-magnetic impurity in graphene

$$\mathbb{G}^{-1}(\tilde{k}, z) = z - \mathbb{t}(\tilde{k}) - (z) = \begin{pmatrix} z - t_{11}(\tilde{k}) - \Sigma_1(z) & -t_{12}(\tilde{k}) & -t_{13}(\tilde{k}) & \dots & -t_{1M}(\tilde{k}) \\ -t_{21}(\tilde{k}) & z - t_{22}(\tilde{k}) - \Sigma_2(z) & -t_{23}(\tilde{k}) & \dots & -t_{2M}(\tilde{k}) \\ -t_{31}(\tilde{k}) & -t_{32}(\tilde{k}) & z - t_{33}(\tilde{k}) - \Sigma_3(z) & \dots & -t_{3M}(\tilde{k}) \\ \vdots & \vdots & \vdots & \ddots & \vdots \\ -t_{M1}(\tilde{k}) & -t_{M2}(\tilde{k}) & -t_{M3}(\tilde{k}) & \dots & z - t_{MM}(\tilde{k}) - \Sigma_M(z) \end{pmatrix}$$



M. Charlebois et al., Phys. Rev. B91, 35132 (2015).

The Dynamical Cluster Approximation

- Based on periodic clusters
- self-consistency condition:

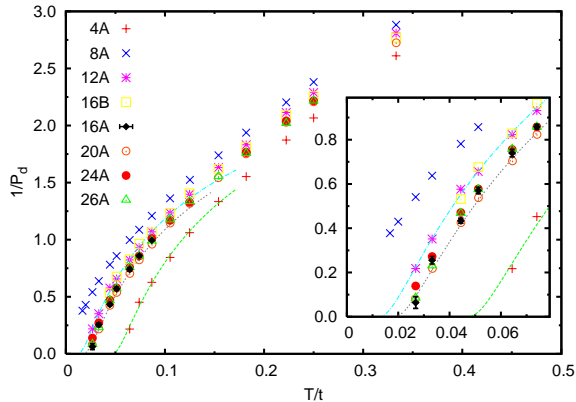
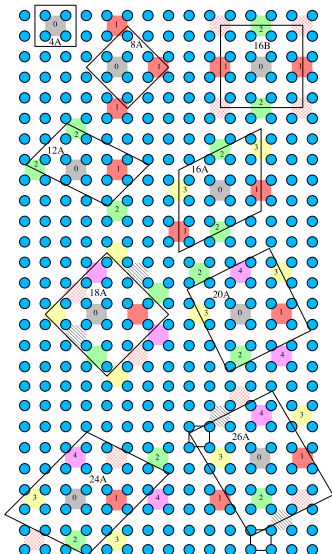
$$\frac{1}{i\omega_n - \bar{t}_K - \Gamma_K(\omega) - \Sigma_K(\omega)} = \frac{L}{N} \sum_{\tilde{k}} \frac{1}{i\omega_n - \varepsilon(\tilde{k} + K) - \Sigma_K(\omega)}$$

where

$$\bar{t}_K = \frac{L}{N} \sum_{\tilde{k}} \varepsilon(\tilde{k} + K)$$

- Not derivable from the Self-energy functional approach
- For large clusters:
 - DCA converges better for $k = 0$ (average) quantities
 - CDMFT converges better for $r = 0$ (local) quantities

DCA on superconductivity



Maier et al., Phys. Rev. Lett. 95, 237001 (2005).

Outline

1 Introduction

2 Dynamical Mean Field Theory

3 Cluster Perturbation Theory

4 Cluster Dynamical Mean Field Theory

5 The self-energy functional approach

- The variational principle
- Calculating the Potthoff functional
- The Variational Cluster Approximation
- Applications
- Optimization
- The (Cluster) Dynamical Impurity Approximation

Motivation

- CPT cannot describe broken symmetry states, because of the finite cluster size
- Idea : add a Weiss field term to the cluster Hamiltonian H' , e.g., for antiferromagnetism:

$$H'_M = M \sum_a e^{iQ \cdot r_a} (n_{a\uparrow} - n_{a\downarrow})$$

$\overrightarrow{\square} (\pi, \pi)$

- This term favors AF order, but does not appear in H , and must be subtracted from V ($H = H' + V$)
- Need a principle to set the value of M : energy minimization?
- Better : Potthoff's self-energy functional approach

The Luttinger-Ward functional

- Luttinger-Ward (or Baym-Kadanoff) functional:

$$\Phi[G] = \text{Diagram 1} + \text{Diagram 2} + \text{Diagram 3} + \dots$$

- Relation with self-energy:

$$\frac{\delta \Phi[G]}{\delta G} = \Sigma$$

- Legendre transform:

↗ functional trace

$$F[\Sigma] = \Phi[G] - \text{Tr}(\Sigma G)$$

$$\frac{\delta F[\Sigma]}{\delta \Sigma} = \frac{\delta \Phi[G]}{\delta G} \frac{\delta G[\Sigma]}{\delta \Sigma} - \Sigma \frac{\delta G[\Sigma]}{\delta \Sigma} - G = -G$$

The variational principle

- Free energy functional:

$$\Omega_t[\Sigma] = F[\Sigma] - \text{Tr} \ln(-G_{0t}^{-1} + \Sigma)$$

- Stationary at the physical self-energy (Euler equation):

$$\frac{\delta \Omega_t[\Sigma]}{\delta \Sigma} = -G + (G_{0t}^{-1} - \Sigma)^{-1} = 0$$

- At the physical self-energy Σ^* , $\Omega_t[\Sigma^*] = \text{grand potential}$
- Approximation strategies with variational principles:
 - Type I : Simplify the Euler equation
 - Type II : Approximate the functional (Hartree-Fock, FLEX)
 - **Type III** : Restrict the variational space, but keep the functional exact

The Reference System

- To evaluate F , use its **universal** character : its functional form depends only on the interaction.
- Introduce a **reference system** H' , which differs from H by one-body terms only (example : the cluster Hamiltonian)
- Suppose H' can be solved exactly. Then, at the physical self-energy Σ of H' ,

$$\Omega' = F[\Sigma] + \text{Tr} \ln(-G')$$

- by eliminating F :

$$\begin{aligned}\Omega_t[\Sigma] &= \Omega' - \text{Tr} \ln(-G') - \text{Tr} \ln(-G_{0t}^{-1} + \Sigma) \\ &= \Omega' - \text{Tr} \ln(-G') + \text{Tr} \ln(-G) \\ &= \Omega' - \text{Tr} \ln(-G') - \text{Tr} \ln(-G'^{-1} + V) \\ &= \Omega' - \text{Tr} \ln(1 - VG')\end{aligned}$$

The Potthoff functional

- Making the trace explicit, one finds

$$\begin{aligned}\Omega_t[\Sigma] &= \Omega' - T \sum_{\omega} \sum_{\tilde{k}} \text{tr} \ln [1 - V(\tilde{k}) G'(\tilde{k}, \omega)] \\ &= \Omega' - T \sum_{\omega} \sum_{\tilde{k}} \ln \det [1 - V(\tilde{k}) G'(\tilde{k}, \omega)]\end{aligned}$$

- The sum over frequencies is to be performed over Matsubara frequencies (or an integral along the imaginary axis at $T = 0$).
- The variation is done over one-body parameters of the cluster Hamiltonian H' .
- In the above example, the solution is found when $\partial \Omega / \partial M = 0$.

Calculating the functional I : exact form

- It can be shown that

$$\text{Tr} \ln(-G) = -T \sum_m \ln(1 + e^{-\beta \omega_m}) + T \sum_m \ln(1 + e^{-\beta \zeta_m})$$

↗ poles of G ↖ zeros of G

- Use the Lehmann representation of the GF:

$$G'_{\alpha\beta}(\omega) = \sum_r \frac{Q_{\alpha r} Q_{\beta r}^*}{\omega - \omega_r} \quad G'(\omega) = Q \frac{1}{\omega - \Lambda} Q^\dagger$$

↳ diagonal(ω_r)

M. Potthoff, Eur. Phys. J. B, 36:335 (2003)

► Lehmann representation

Calculating the functional I : exact form (2)

- A similar representation holds for the CPT Green function

$$\begin{aligned} G(\tilde{k}, \omega) &= \frac{1}{G'^{-1} - V(\tilde{k})} = \frac{1}{[Q_{\omega-\Lambda}^{-1} Q^\dagger]^{-1} - V(\tilde{k})} \\ &= Q \frac{1}{\omega - L(\tilde{k})} Q^\dagger \quad L(\tilde{k}) = \Lambda + Q^\dagger V(\tilde{k}) Q \end{aligned}$$

- Let $\omega_r(\tilde{k})$ be the eigenvalues of $L(\tilde{k})$, i.e., the poles of $G(\tilde{k}, \omega)$. Then

variational parameters ↪

$$\Omega(x) = \Omega'(x) - \sum_{\omega'_r < 0} \omega'_r + \frac{L}{N} \sum_{\tilde{k}} \sum_{\omega_r(\tilde{k}) < 0} \omega_r(\tilde{k})$$

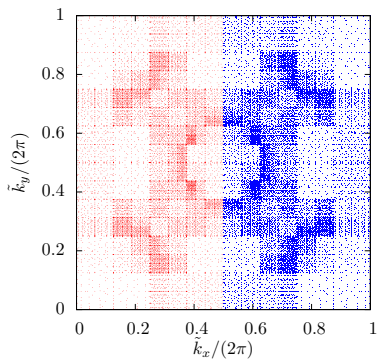
- Note: the zeros of G' and G are the same, since they have the same self-energy.

M. Aichhorn et al., Phys. Rev. B 74 : 235117 (2006)

Calculating the functional II : numerical integral

Except for very small clusters ($L \sim 4$), it is much faster to perform a numerical integration over frequencies:

$$\Omega(x) = \Omega'(x) - \int_0^\infty \frac{d\omega}{\pi} \frac{L}{N} \sum_{\tilde{k}} \ln \left| \det(1 - V(\tilde{k}) G'(i\omega)) \right| - L(\mu - \mu')$$



The integral must be done using an adaptive method that refines a mesh where necessary.

For instance: The **CUBA** library

<http://www.feynarts.de/cuba/>

Grid of 17,095 points used in an adaptive integration over wavevectors

The variational Cluster Approximation: procedure

- 1 Set up a superlattice of clusters
- 2 Choose a set of variational parameters, e.g. Weiss fields for broken symmetries
- 3 Set up the calculation of the Potthoff functional:
- 4 Use an optimization method to find the stationary points
 - E.g. the Newton-Raphson method, or a quasi-Newton method
- 5 Adopt the cluster self-energy associated with the stationary point with the lowest Ω and use it as in CPT or CDMFT.
- 6 Adopt the value of Ω as the best estimate of the grand potential

VCA vs Mean-Field Theory

- Differs from Mean-Field Theory:
 - Interaction is left intact, it is not factorized
 - Retains exact short-range correlations
 - Weiss field \neq order parameter
 - More stringent than MFT
 - Controlled by the cluster size
- Similarities with MFT:
 - No long-range fluctuations (no disorder from Goldstone modes)
 - Yet : no LRO for Néel AF in one dimension
 - Need to compare different orders
 - yet : they may be placed in competition / coexistence

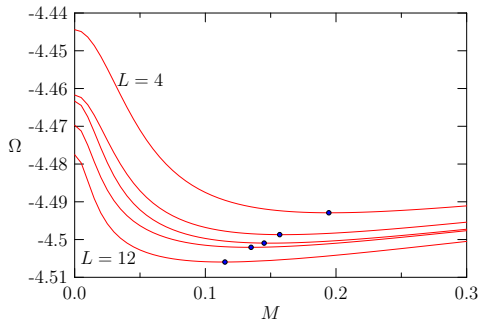
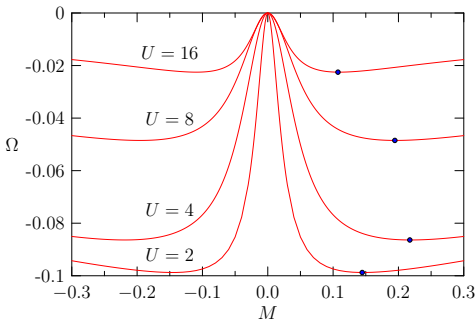
Application: Néel Antiferromagnetism

- Used the Weiss field

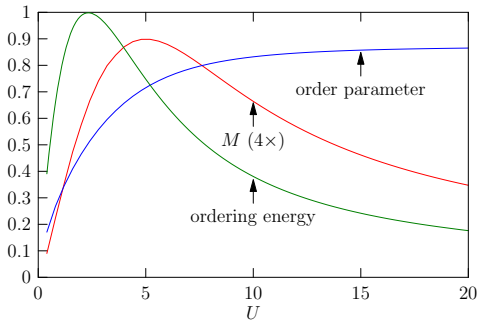
↗ (π, π)

$$H'_M = M \sum_{\mathbf{r}} e^{iQ \cdot \mathbf{r}} (n_{\mathbf{r}\uparrow} - n_{\mathbf{r}\downarrow})$$

- Profile of Ω for the half-filled, square lattice Hubbard model:

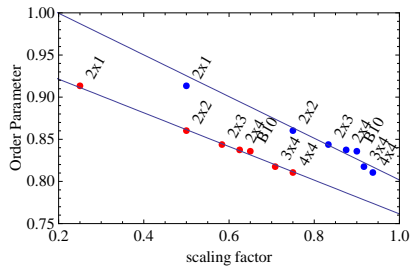
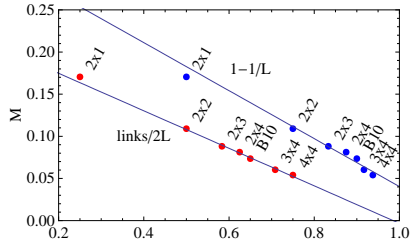


Néel Antiferromagnetism (cont.)



Best scaling factor :

$$q = \frac{\text{number of links}}{2 \times \text{number of sites}}$$



Application: Superconductivity

- Need to add a pairing field

$$\Delta = \sum_{\mathbf{r}, \mathbf{r}'} \Delta_{\mathbf{r}\mathbf{r}'} c_{\mathbf{r}\uparrow} c_{\mathbf{r}'\downarrow} + \text{H.c}$$

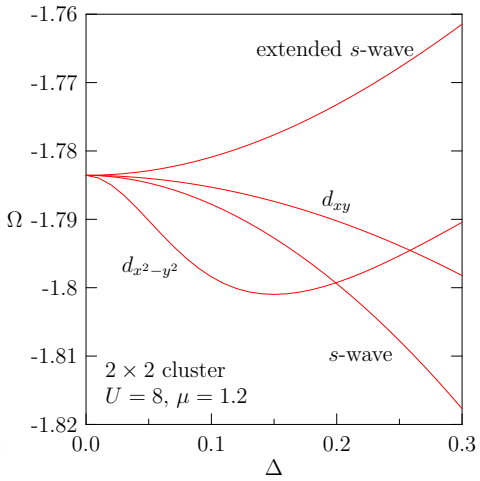
- s -wave pairing: $\Delta_{\mathbf{r}\mathbf{r}'} = \delta_{\mathbf{r}\mathbf{r}'}$

- $d_{x^2-y^2}$ pairing:

$$\Delta_{\mathbf{r}\mathbf{r}'} = \begin{cases} \begin{cases} 1 & \text{if } \mathbf{r} - \mathbf{r}' = \pm \mathbf{x} \\ -1 & \text{if } \mathbf{r} - \mathbf{r}' = \pm \mathbf{y} \end{cases} \end{cases}$$

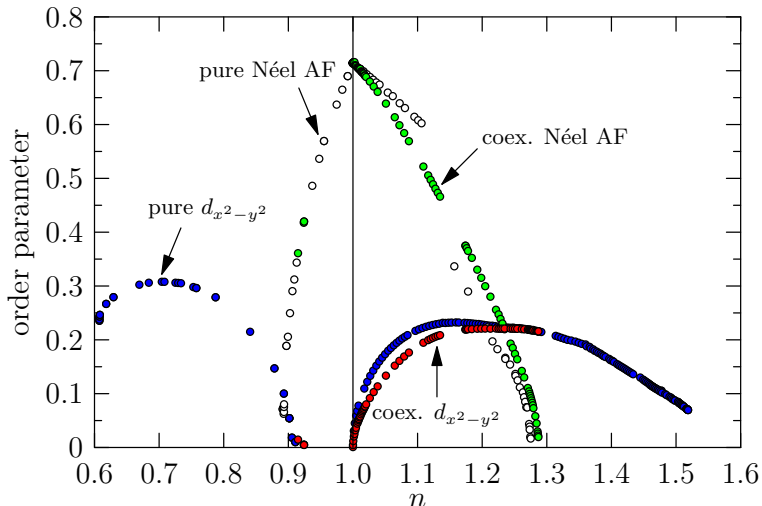
- d_{xy} pairing:

$$\Delta_{\mathbf{r}\mathbf{r}'} = \begin{cases} \begin{cases} 1 & \text{if } \mathbf{r} - \mathbf{r}' = \pm(\mathbf{x} + \mathbf{y}) \\ -1 & \text{if } \mathbf{r} - \mathbf{r}' = \pm(\mathbf{x} - \mathbf{y}) \end{cases} \end{cases}$$

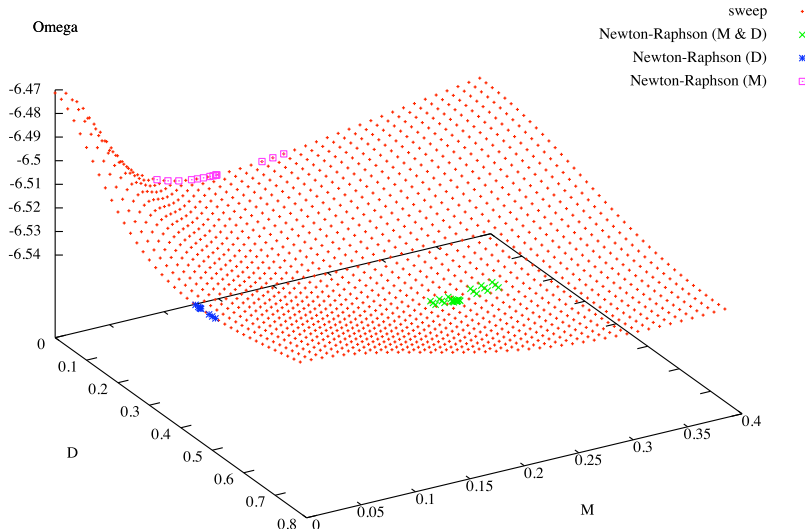


Competing SC and AF orders

- One-band Hubbard model for the cuprates: $t' = -0.3$, $t'' = 0.2$, $U = 8$:



Example: Homogeneous coexistence of dSC and AF orders



Optimization procedure

- Need to find the stationary points of $\Omega(x)$ with as few evaluations as possible
- Example: the **Newton-Raphson** method:
 - Evaluate Ω at a number of points at and around x_0 that just fits a quadratic form
 - Move to the stationary point x_1 of that quadratic form and repeat
 - Stop when $|x_i - x_{i-1}|$, or the numerical gradient $|\nabla\Omega|$, converges
 - Not robust : it converges fast when started close enough to the solution, but it can err...
- Proceed adiabatically through external parameter space
(e.g. as function of U or μ)

The (Cluster) Dynamical Impurity Approximation (CDIA)

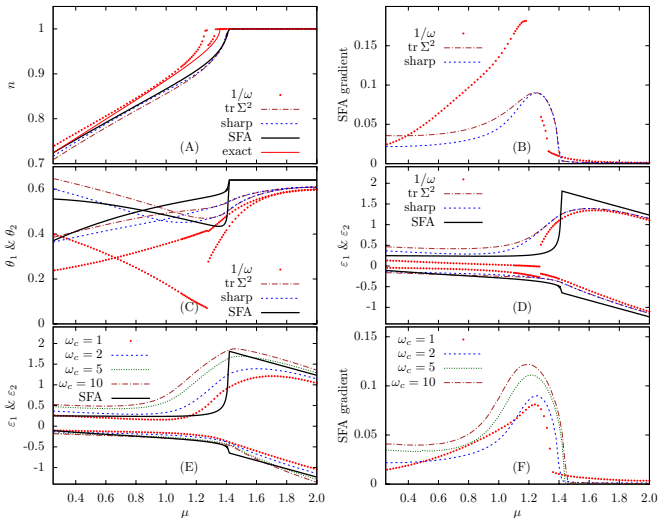
- The bath parameters (ε_μ , $\theta_{a\mu}$, etc) are variational parameters
- The bath makes a contribution to the Potthoff functional:

$$\Omega_{\text{bath}} = \sum_{\varepsilon_\alpha < 0} \varepsilon_\alpha$$

- One can in principle use the same procedure as in VCA...
- ...but in practice it is more difficult.
- The presence of the bath increases the resolution of the approach in the time domain, at the cost of spatial resolution, for a fixed total number of orbitals (cluster + bath).
- Euler equations for the stationary point:

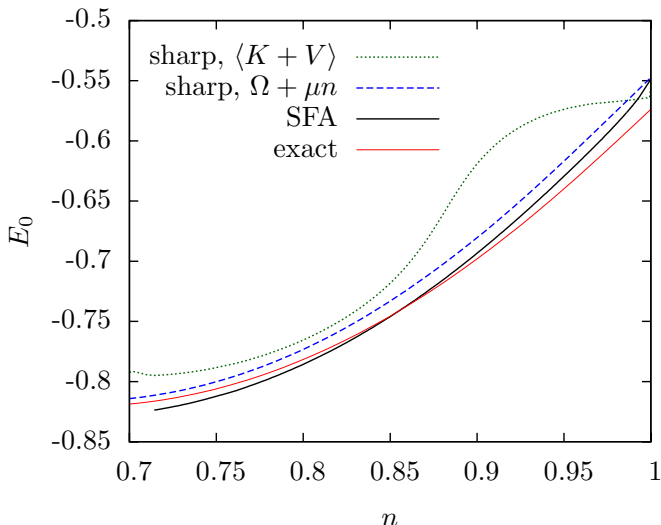
$$\sum_{\omega_n} \text{tr} \left\{ \left[G'(i\omega_n) - \bar{G}(i\omega_n) \right] \cdot \frac{\partial \Sigma'(i\omega_n)}{\partial \theta} \right\} = 0.$$

The 1D Hubbard model

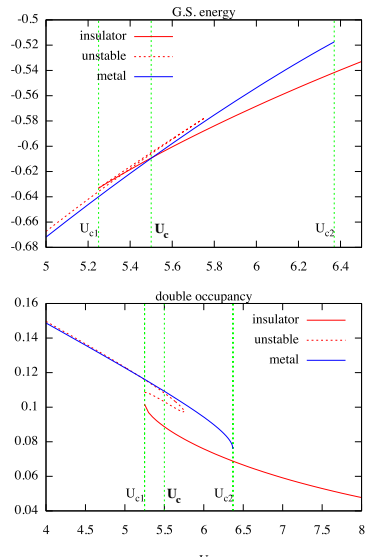
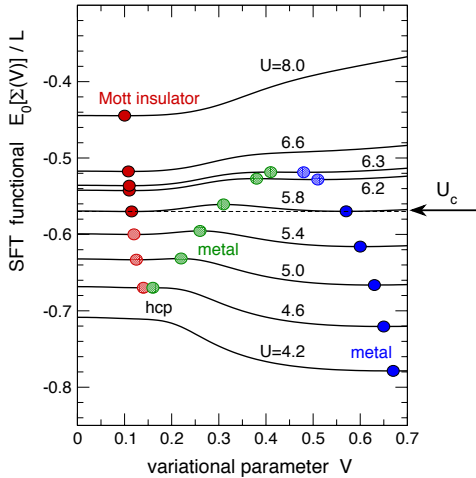


The 1D Hubbard model (cont.)

Ground state energy as a function of doping ($U = 4t$)



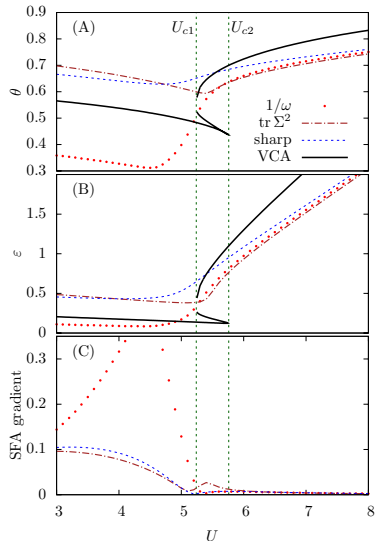
First-order character of the Mott transition (CDIA)



Mott transition (CDIA vs CDMFT)

- The Mott transition may not show up as first-order in CDMFT, even though it is in the CDIA
- The choice of distance function matters

D. Sénéchal, Phys. Rev. B 81 (2010), 235125.



Outline

1 Introduction

2 Dynamical Mean Field Theory

3 Cluster Perturbation Theory

4 Cluster Dynamical Mean Field Theory

5 The self-energy functional approach

6 Exact Diagonalizations

- The Hilbert space
- Coding the states
- The Lanczos method
- Calculating the Green function

Exact diagonalizations vs Quantum Monte Carlo

	ED	QMC
temperature	$T = 0$	$T > 0$
frequencies	real/complex	complex
sign problem	no	yes
system size	small	moderate
CDMFT bath	small	infinite
interaction strength	any	depends on expansion scheme

The exact diagonalization procedure

- 1 Build a basis
- 2 Construct the Hamiltonian matrix (stored or not)
- 3 Find the ground state (e.g. by the Lanczos method)
 - Calculate ground state properties (expectation values, etc.)
- 4 Calculate a representation of the one-body Green function:
 - Continuous-fraction representation
 - Lehmann representation
- 5 Calculate dynamical properties from the Green function

The Hubbard model on a cluster of size L

- N_\uparrow and N_\downarrow separately conserved in the simple Hubbard model
- Dimension of the Hilbert space (half-filling):

$$d = \left(\frac{L!}{[(L/2)!]^2} \right)^2 \sim 2 \frac{4^L}{\pi L}$$

- $L = 16$: One double-precision vector requires 1.23 GB of memory

L	dimension
2	4
4	36
6	400
8	4 900
10	63 504
12	853 776
14	11 778 624
16	165 636 900

Two-site cluster: Hamiltonian matrix

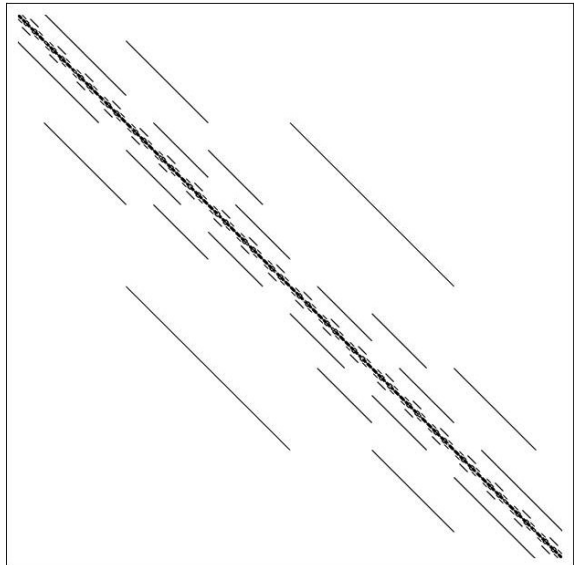
- Half-filled, two-site Hubbard model: 4 states
- States and Hamiltonian matrix:

$$\begin{array}{l} |01,01\rangle \\ |01,10\rangle \\ |10,01\rangle \\ |10,10\rangle \end{array} \left(\begin{array}{cccc} U - 2\mu & -t & -t & 0 \\ -t & -2\mu & 0 & -t \\ -t & 0 & -2\mu & -t \\ 0 & -t & -t & U - 2\mu \end{array} \right)$$

spin \uparrow occupation \leftarrow \rightarrow spin \downarrow occupation

Six-site cluster: Hamiltonian matrix

Sparse matrix structure
 400×400



Coding the states

- Tensor product structure of the Hilbert space: $V = V_{N_\uparrow} \otimes V_{N_\downarrow}$
- dimension:

$$d = d(N_\uparrow)d(N_\downarrow) \quad d(N_\sigma) = \frac{L!}{N_\sigma!(L - N_\sigma)!}$$

- Example (6 sites):

	0	1	2	3	4	5	6
0	1	6	15	20	15	6	1
1	6	36	90	120	90	36	6
2	15	90	225	300	225	90	15
3	20	120	300	400	300	120	20
4	15	90	225	300	225	90	15
5	6	36	90	120	90	36	6
6	1	6	15	20	15	6	1

Coding the states (2)

- Basis of occupation number eigenstates:

$$(c_{1\uparrow}^\dagger)^{n_{1\uparrow}} \cdots (c_{L\uparrow}^\dagger)^{n_{L\uparrow}} (c_{1\downarrow}^\dagger)^{n_{1\downarrow}} \cdots (c_{L\downarrow}^\dagger)^{n_{L\downarrow}} |0\rangle \quad n_{i\sigma} = 0 \text{ or } 1$$

- Correspondence with binary representation of integers:

$$b_\sigma = (n_{1\sigma} n_{2\sigma} \cdots n_{L\sigma})_2$$

- For a given $(N_\uparrow, N_\downarrow)$, we need a direct table:

$$b_\uparrow = B_\uparrow(i_\uparrow) \quad b_\downarrow = B_\downarrow(i_\downarrow)$$

- ...and a reverse table:

$$i = I_\uparrow(b_\uparrow) + d_{N\uparrow} I_\downarrow(b_\downarrow) \quad i_\uparrow = i \% d_{N\uparrow} \quad i_\downarrow = i / d_{N\uparrow}$$

↗ consecutive label mod ↙ ↗ int. division

Constructing the Hamiltonian matrix

- Form of Hamiltonian:

$$H = K_{\uparrow} \otimes 1 + 1 \otimes K_{\downarrow} + V_{\text{int.}} \quad K = \sum_{a,b} t_{ab} c_a^{\dagger} c_b$$

- K is stored in sparse form.
- $V_{\text{int.}}$ is diagonal and is stored.
- Matrix elements of $V_{\text{int.}}$: `bit_count(b_{\uparrow} & b_{\downarrow})`
- Two basis states $|b_{\sigma}\rangle$ and $|b'_{\sigma}\rangle$ are connected with the matrix K if their binary representations differ at two positions a and b .

$$\langle b' | K | b \rangle = (-1)^{M_{ab}} t_{ab} \quad M_{ab} = \sum_{c=a+1}^{b-1} n_c$$

- We find it practical to construct and store all terms of the Hamiltonian separately.

The Lanczos method

- Finds the lowest eigenpair by an iterative application of H
- Start with random vector $|\phi_0\rangle$
- An iterative procedure builds the Krylov subspace:

$$\mathcal{K} = \text{span}\{|\phi_0\rangle, H|\phi_0\rangle, H^2|\phi_0\rangle, \dots, H^M|\phi_0\rangle\}$$

- Lanczos three-way recursion for an orthogonal basis $\{|\phi_n\rangle\}$:

$$|\phi_{n+1}\rangle = H|\phi_n\rangle - a_n|\phi_n\rangle - b_n^2|\phi_{n-1}\rangle$$
$$a_n = \frac{\langle\phi_n|H|\phi_n\rangle}{\langle\phi_n|\phi_n\rangle} \quad b_n^2 = \frac{\langle\phi_n|\phi_n\rangle}{\langle\phi_{n-1}|\phi_{n-1}\rangle} \quad b_0 = 0$$

The Lanczos method (2)

- In the basis of normalized states $|n\rangle = |\phi_n\rangle / \sqrt{\langle \phi_n | \phi_n \rangle}$, the projected Hamiltonian has the tridiagonal form

projector onto $\mathcal{K} \leftarrow$

$$PHP = T = \begin{pmatrix} a_0 & b_1 & 0 & 0 & \cdots & 0 \\ b_1 & a_1 & b_2 & 0 & \cdots & 0 \\ 0 & b_2 & a_2 & b_3 & \cdots & 0 \\ \vdots & \vdots & \vdots & \vdots & \ddots & \vdots \\ 0 & 0 & 0 & 0 & \cdots & a_N \end{pmatrix}$$

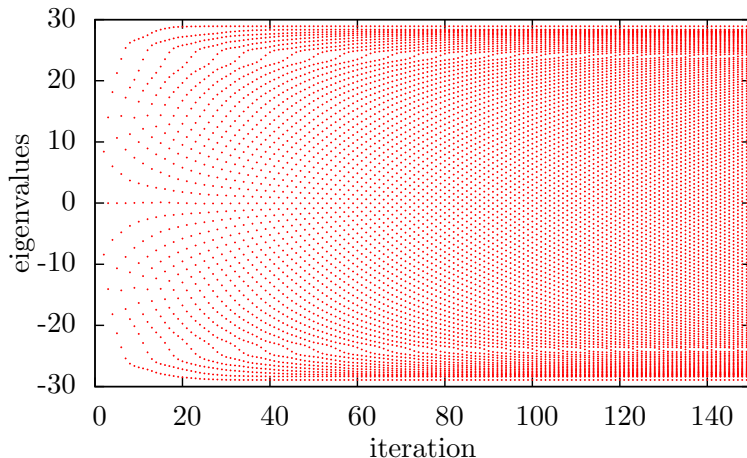
- At each step n , find the lowest eigenvalue of that matrix
- Stop when the estimated Ritz residual $\|T|\psi\rangle - E_0|\psi\rangle\|$ is small enough
- Run again to find eigenvector $|\psi\rangle = \sum_n \psi_n |n\rangle$ as the $|\phi_n\rangle$'s are not kept in memory.

The Lanczos method: features

- Required number of iterations: typically from 50 to 200
- Extreme eigenvalues converge first
- Rate of convergence increases with separation between ground state and first excited state
- Cannot resolve degenerate ground states : only one state per ground state manifold is picked up
- If one is interested in low lying states, re-orthogonalization may be required, as orthogonality leaks will occur. But then Lanczos intermediate states need to be stored.
- For degenerate ground states and low lying states (e.g. in DMRG), the Davidson method is generally preferable

The Lanczos method: illustration of the convergence

149 iterations on a matrix of dimension 213,840: eigenvalues of the tridiagonal projection as a function of iteration step



Lanczos method for the Green function

- Zero temperature Green function:

$$G_{\alpha\beta}(z) = G_{\alpha\beta}^{(e)}(z) + G_{\alpha\beta}^{(h)}(z)$$

$$G_{\alpha\beta}^{(e)}(z) = \langle \Omega | c_\alpha \frac{1}{z - H + E_0} c_\beta^\dagger | \Omega \rangle$$

$$G_{\alpha\beta}^{(h)}(z) = \langle \Omega | c_\beta^\dagger \frac{1}{z + H - E_0} c_\alpha | \Omega \rangle$$

- Consider the diagonal element

$$|\phi_\alpha\rangle = c_\alpha^\dagger |\Omega\rangle \implies G_{\alpha\alpha}^{(e)} = \langle \phi_\alpha | \frac{1}{z - H + E_0} | \phi_\alpha \rangle$$

- Use the expansion

$$\frac{1}{z - H} = \frac{1}{z} + \frac{1}{z^2} H + \frac{1}{z^3} H^2 + \dots$$

Lanczos method for the Green function (2)

- Truncated expansion evaluated exactly in Krylov subspace generated by $|\phi_\alpha\rangle$ if we perform a Lanczos procedure on $|\phi_\alpha\rangle$.
- Then $G_{\alpha\alpha}^{(e)}$ is given by a Jacobi continued fraction:

$$G_{\alpha\alpha}^{(e)}(z) = \frac{\langle \phi_\alpha | \phi_\alpha \rangle}{z - a_0 - \cfrac{b_1^2}{z - a_1 - \cfrac{b_2^2}{z - a_2 - \dots}}}$$

- The coefficients a_n and b_n are stored in memory
- What about non diagonal elements $G_{\alpha\beta}^{(e)}$?

See, e.g., E. Dagotto, Rev. Mod. Phys. 66:763 (1994)

Lanczos method for the Green function (3)

- Trick: Define the combination

$$G_{\alpha\beta}^{(e)+}(z) = \langle \Omega | (c_\alpha + c_\beta) \frac{1}{z - H + E_0} (c_\alpha + c_\beta)^\dagger | \Omega \rangle$$

- $G_{\alpha\beta}^{(e)+}(z)$ can be calculated like $G_{\alpha\alpha}^{(e)}(z)$
- Since $G_{\alpha\beta}^{(e)}(z) = G_{\beta\alpha}^{(e)}(z)$, then

$$G_{\alpha\beta}^{(e)}(z) = \frac{1}{2} \left[G_{\alpha\beta}^{(e)+}(z) - G_{\alpha\alpha}^{(e)}(z) - G_{\beta\beta}^{(e)}(z) \right]$$

- Likewise for $G_{\alpha\beta}^{(h)}(z)$

The Lehmann representation

$$G_{\alpha\beta}(z) = \sum_m \frac{\langle \Omega | c_\alpha | m \rangle \langle m | c_\beta^\dagger | \Omega \rangle}{z - E_m + E_0} + \sum_n \frac{\langle \Omega | c_\beta^\dagger | n \rangle \langle n | c_\alpha | \Omega \rangle}{z + E_n - E_0}$$

Define the matrices

$$Q_{\alpha m}^{(e)} = \langle \Omega | c_\alpha | m \rangle \quad Q_{\alpha n}^{(h)} = \langle \Omega | c_\alpha^\dagger | n \rangle$$

Then

$$\begin{aligned} G_{\alpha\beta}(z) &= \sum_m \frac{Q_{\alpha m}^{(e)} Q_{\beta m}^{(e)*}}{z - \omega_m^{(e)}} + \sum_n \frac{Q_{\alpha n}^{(h)} Q_{\beta n}^{(h)*}}{z - \omega_n^{(h)}} \\ &= \sum_r \frac{Q_{\alpha r} Q_{\beta r}^*}{z - \omega_r} \quad QQ^\dagger = 1 \end{aligned}$$

The Band Lanczos method

- Define $|\phi_\alpha\rangle = c_\alpha^\dagger |\Omega\rangle$, $\alpha = 1, \dots, L$.
- Extended Krylov space :

$$\{|\phi_1\rangle, \dots, |\phi_L\rangle, H|\phi_1\rangle, \dots, H|\phi_L\rangle, \dots, (H)^M|\phi_1\rangle, \dots, (H)^M|\phi_L\rangle\}$$

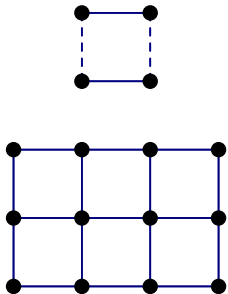
- States are built iteratively and orthogonalized
- Possible linearly dependent states are eliminated ('deflation')
- A band representation of the Hamiltonian ($2L + 1$ diagonals) is formed in the Krylov subspace.
- It is diagonalized and the eigenpairs are used to build an approximate Lehmann representation

<http://www.cs.utk.edu/dongarra/etemplates/node131.html>

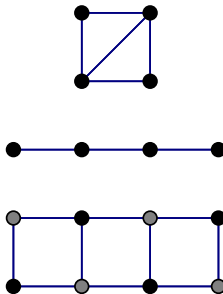
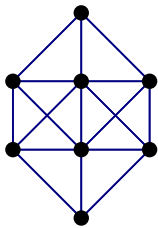
Lanczos vs band Lanczos

- The usual Lanczos method for the Green function needs 3 vectors in memory, and $L(L + 1)$ distinct Lanczos procedures.
- The band Lanczos method requires $3L + 1$ vectors in memory, but requires only 2 iterative procedures ((e) et (h)).
- If Memory allows it, the band Lanczos is much faster.

Cluster symmetries



Clusters with C_{2v} symmetry



Clusters with C_2 symmetry

Cluster symmetries (2)

- Symmetry operations form a **group** \mathfrak{G}
- The most common occurrences are :
 - C_1 : The trivial group (no symmetry)
 - C_2 : The 2-element group (e.g. left-right symmetry)
 - C_{2v} : 2 reflections, 1 π -rotation
 - C_{4v} : 4 reflections, 1 π -rotation, 2 $\pi/2$ -rotations
 - C_{3v} : 3 reflections, 3 $2\pi/3$ -rotations
 - C_{6v} : 6 reflections, 1 π , 2 $\pi/3$, 2 $\pi/6$ rotations
- States in the Hilbert space fall into a finite number of irreducible representations (irreps) of \mathfrak{G}
- The Hamiltonian H' is block diagonal w.r.t. to irreps.
- Easiest to implement with Abelian (i.e. commuting) groups

Taking advantage of cluster symmetries...

→ order of the group

- Reduces the dimension of the Hilbert space by $\sim |\mathfrak{G}|$
- Accelerates the convergence of the Lanczos algorithm
- Reduces the number of Band Lanczos starting vectors by $|\mathfrak{G}|$
- But: complicates coding of the basis states
- Make use of the projection operator:

dimension of irrep. ←

$$P^{(\alpha)} = \frac{d_\alpha}{|\mathfrak{G}|} \sum_{g \in \mathfrak{G}} \chi_g^{(\alpha)*} g$$

group character

See, e.g. Poilblanc & Laflorencie cond-mat/0408363

Group characters

C_2	E	C_2
A	1	1
B	1	-1

C_{2v}	e	c_2	σ_1	σ_2
A_1	1	1	1	1
A_2	1	1	-1	-1
B_1	1	-1	1	-1
B_2	1	-1	-1	1

C_{4v}	e	c_2	$2c_4$	$2\sigma_1$	$2\sigma_2$
A_1	1	1	1	1	1
A_2	1	1	1	-1	-1
B_1	1	1	-1	1	-1
B_2	1	1	-1	-1	1
E	2	-2	0	0	0

Taking advantage of cluster symmetries (2)

- Need new basis states, made of sets of binary states related by the group action:

$$|\psi\rangle = \frac{d_\alpha}{|\mathfrak{G}|} \sum_g \chi_g^{(\alpha)*} g|b\rangle \quad g|b\rangle = \phi_g(b)|gb\rangle$$

↗ fermionic phase

- Then matrix elements take the form

$$\langle\psi_2|H|\psi_1\rangle = \frac{d_\alpha}{|\mathfrak{G}|} \sum_g \chi_h^{(\alpha)*} \phi_g(b) \langle gb_2|H|b_1\rangle$$

- When computing the Green function, one needs to use combinations of creation operators that fall into group representations. For instance (4×1):

$$\begin{aligned} c_1^{(A)} &= c_1 + c_4 & c_1^{(B)} &= c_1 - c_4 & \circ & \text{---} & \circ & \text{---} & \circ & \text{---} & \circ \\ c_2^{(A)} &= c_2 + c_3 & c_2^{(B)} &= c_2 - c_3 & 1 & & 2 & & 3 & & 4 \end{aligned}$$

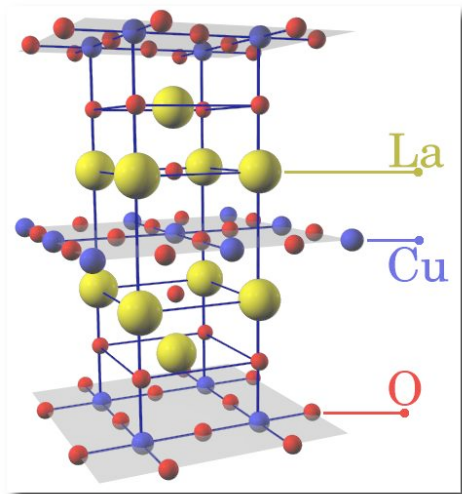
Taking advantage of cluster symmetries (3)

Example : number of matrix elements of the kinetic energy operator (Nearest neighbor) on a 3×4 cluster with C_{2v} symmetry:

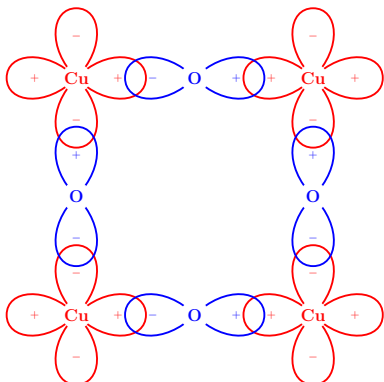
dim. value	A_1 213,840	A_2 213,248	B_1 213,440	B_2 213,248
-2	96	736	704	0
$-\sqrt{2}$	12,640	6,208	7,584	5,072
-1	2,983,264	2,936,144	2,884,832	2,911,920
1	952,000	997,168	1,050,432	1,021,392
$\sqrt{2}$	5,088	2,304	3,232	2,992
2	32	0	0	0

QUESTIONS ?

High- T_c superconductors : structure



Physics of CuO₂ planes



Three-band model for HTSC

- A Hubbard model involving the three orbitals is (Emery 1987)

$$\begin{aligned} H = & (\varepsilon_d - \mu) \sum_{r,\sigma} n_{r\sigma}^{(d)} + (\varepsilon_p - \mu) \sum_{x,\sigma} n_{x\sigma}^{(p)} \\ & + t_{pd} \sum_{\langle r,x \rangle} (p_{x\sigma}^\dagger d_{r\sigma} + d_{r\sigma}^\dagger p_{x\sigma}) + t_{pp} \sum_{\langle x,x' \rangle} (p_{x\sigma}^\dagger p_{x'\sigma} + \text{H.c.}) \\ & + U_d \sum_r n_{r\uparrow}^{(d)} n_{r\downarrow}^{(d)} + U_p \sum_x n_{x\uparrow}^{(p)} n_{x\downarrow}^{(p)} + U_{pd} \sum_{\langle r,x \rangle} n_r^{(d)} n_x^{(p)} \end{aligned}$$

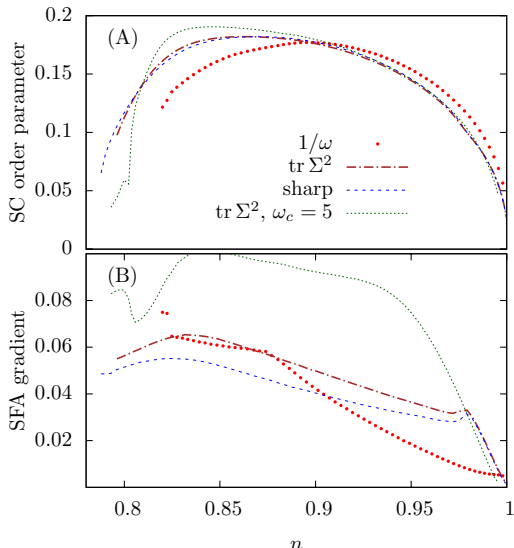
- with the parameters (in eV, from LDA, in the hole representation)

$\varepsilon_p - \varepsilon_d$	t_{pd}	t_{pp}	U_d	U_p	U_{pd}
3.6	1.3	0.65	10.5	4	1.2

Effect of the distance function

- What weights $W(i\omega_n)$ to use?
- $W \sim 1/\omega$ better in the underdoped region
- Sharp cutoff better in the overdoped region

D. Sénéchal, Phys. Rev. B 81 (2010), 235125.



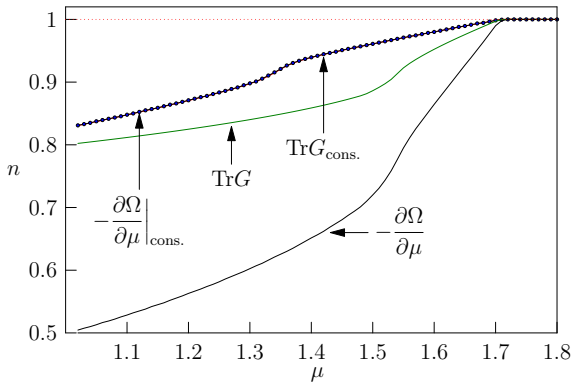
Thermodynamic consistency

The electron density n may be calculated either as

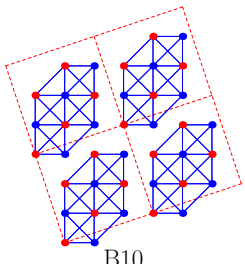
$$n = \text{Tr}G \quad \text{or} \quad n = -\frac{\partial \Omega}{\partial \mu}$$

The two methods give different results, except if the cluster chemical potential μ' is a variational parameter

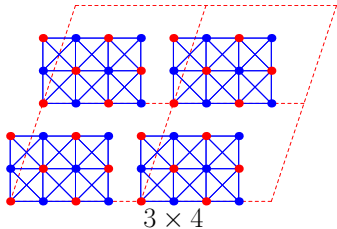
2×2 cluster
 $U = 8$
normal state



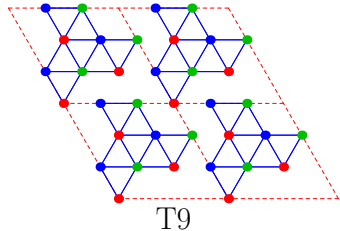
Example clusters



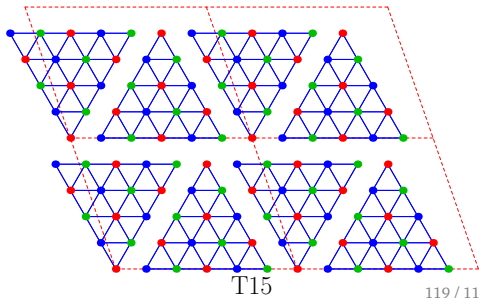
B10



3×4



T9



T15